DESIGN AND ANALYSIS OF ULTRA-WIDEBAND (UWB) PRINTED MONOPOLE ANTENNAS OF CIRCULAR SHAPE

A THESIS SUBMITTED TO
THE GRADUATE SCHOOL OF NATURAL AND APPLIED SCIENCES
OF
MIDDLE EAST TECHNICAL UNIVERSITY

BY

SERKAN KARADAĞ

IN PARTIAL FULFILLMENT OF THE REQUIREMENTS
FOR
THE DEGREE OF MASTER OF SCIENCE
IN
ELECTRICAL AND ELECTRONICS ENGINEERING

NOVEMBER 2017

Approval of the thesis:

DESIGN AND ANALYSIS OF ULTRA-WIDEBAND (UWB) PRINTED MONOPOLE ANTENNAS OF CIRCULAR SHAPE

submitted by **SERKAN KARADAĞ** in partial fulfillment of the requirement for the degree of **Master of Science in Electrical and Electronics Engineering Department, Middle East Technical University** by,

Prof. Dr. Gülbin Dural Ünver _____
Dean, Graduate School of **Natural and Applied Sciences**

Prof. Dr. Tolga Çiloğlu _____
Head of Department, **Electrical and Electronics Engineering**

Prof. Dr. Özlem Aydın Çivi _____
Supervisor, **Electrical and Electronics Engineering**

Examining Committee Members:

Prof. Dr. Sencer Koç _____
Electrical and Electronics Engineering Dept., METU

Prof. Dr. Özlem Aydın Çivi _____
Electrical and Electronics Engineering Dept., METU

Assoc. Prof. Dr. Lale Alatan _____
Electrical and Electronics Engineering Dept., METU

Assoc. Prof. Dr. Özgür Ergül _____
Electrical and Electronics Engineering Dept., METU

Prof. Dr. Birsen Saka _____
Electrical and Electronics Eng. Dept., Hacettepe University

Date: 15.11.2017

I hereby declare that all information in this document has been obtained and presented in accordance with academic rules and ethical conduct. I also declare that, as required by these rules and conduct, I have fully cited and referenced all material and results that are not original to this work.

Name, Last name: Serkan Karadağ

Signature:

ABSTRACT

DESIGN AND ANALYSIS OF ULTRA-WIDEBAND (UWB) PRINTED MONOPOLE ANTENNAS OF CIRCULAR SHAPE

Karadağ, Serkan

M. Sc., Department of Electrical and Electronics Engineering

Supervisor: Prof Dr. Özlem Aydın Çivi

November 2017, 76 Pages

This study proposes three microstrip line fed circular monopole antennas with ultra-wideband (UWB) characteristics, improved omnidirectional radiation pattern and WLAN (5 GHz-6 GHz) band notched characteristics for wireless and mobile communication systems.

In this thesis, first, a microstrip line fed ultra-wideband ring monopole antenna with improved omnidirectional radiation pattern is designed, fabricated and measured. Two corners are tapered on the ground plane for increasing impedance bandwidth. In order to obtain low cross polarization level on the H plane, two symmetrical rectangular notches are cut on lower side of the ground plane. Moreover, in the center of the circular patch, a slot is opened to improve impedance matching at lower frequencies. The proposed antenna has measured bandwidth from 2.6 GHz to 20 GHz. The antenna has omnidirectional radiation pattern on the H-plane. The measured cross polarization level is low up to 9 GHz on the H plane. Moreover, it has near-omnidirectional radiation pattern on the E-plane. The measured cross polarization is low at all frequencies on the E-plane.

Secondly, an UWB antenna (4.3 GHz-11.2 GHz) with symmetrically located open-circuited stubs is designed, fabricated and measured. The aim of this design is to distribute some part of the current in the symmetrical open circuited stubs to

improve the radiation patterns of the antenna at high frequencies. The cross polarization level is less than -20 dB up to 6 GHz. However, cross polarization level increases at high frequencies.

Finally, an UWB with band-notched characteristics (WLAN 5 GHz-6.1 GHz) is designed, fabricated and measured. U shaped slot is etched on feedline to obtain band-notched characteristics. Antenna shows omnidirectional pattern on the H plane up to 7 GHz. The cross polarization level is below -20 dB up to 7 GHz. The proposed antenna has measured bandwidth from 2.5 GHz to 16.5 GHz. The antenna has wide bandwidth and large peak gain when compared to the previous studies.

For all antennas developed, the effect of different parameters such as the gap between monopole patch and ground plane, width of ground plane, length of the ground plane, dielectric constant, thickness, and patch radius is studied. Measured return loss characteristics and radiation patterns agree well with the simulated ones.

Keywords: printed circular monopole antenna, omnidirectional antenna, low-cross polarization ultra-wide bandwidth, band notched monopole antenna, high gain monopole antenna

ÖZ

HALKA ŞEKLİNDEKİ GENİŞ BANTLI MONOPOL ANTENLERİN TASARIMI VE ANALİZİ

Karadağ, Serkan
Yüksek Lisans, Elektrik ve Elektronik Mühendisliği Bölümü
Tez Yöneticisi: Prof. Dr. Özlem Aydın Çivi

Kasım 2017, 76 Sayfa

Bu çalışma ile kablosuz ve mobil haberleşme sistemleri için üç adet geniş bantlı, her yönde yayın yapabilen ve 5 GHz-6 GHz WLAN bandında söndürme özelliği olan monopol antenler tasarlanmıştır.

Bu tezde ilk olarak halka, mikroşerit beslemeli, geniş bantlı (2.6 GHz-20 GHz) ve her yönde yayın yapabilen anten tasarlanmış, üretilmiş ve ölçüm alınmıştır. H düzleminde çapraz polarizasyon seviyesi 9 GHz e kadar -20 dB'den düşüktür. Empedans bant genişliğini artırmak amacıyla zemin yüzeyin üst köşeleri kesilmiştir. Çapraz polarizasyonu azaltmak için zemin yüzeyin alt taraflarında simetrik dikdörtgen yarıklar açılmıştır. Ayrıca, düşük frekanslarda empedans uyumunu iyileştirmek için anten merkezinde halka açılmıştır.

İkinci olarak, geniş bantlı (4.3 GHz-11.2 GHz) simetrik parallel tıknazlı anten tasarlanmıştır. Bu tasarımın amacı akımın bir kısmını tıknazlara dağıtarak yüksek frekanslardaki ışınım desenini geliştirmektir. H düzleminde ölçülen çapraz polarizasyon seviyesinin 6 GHz'e kadar -20 dB'den az olduğu gözlemlenmiştir. 6 GHz üstünde çapraz polarizasyon seviyesi artmaktadır.

Son olarak da geniş bantlı (2.5 GHz-16 GHz) ve (WLAN 5 GHz-6.1 GHz) söndürme özelliği olan bir anten tasarlanmış, üretilmiş ve ölçüm alınmıştır. Besleme hattı üzerinde, U şeklinde yarık açılarak antene söndürme özelliği

kazandırılmıştır. Anten H düzleminde 7 GHz'e kadar her yönde yayın yapabilmektedir. H düzleminde çapraz polarizasyon seviyesi 7 GHz'e kadar -20 dB'den küçüktür.

Geliştirilen tüm antenler için anten ile zemin arasındaki açıklık, zemin genişliği, zemin uzunluğu, dielektrik katsayısı, kalınlık ve yarıçap gibi parametrelerin anten performansına olan etkisine bakılmıştır. Simülasyon sonuçlarında elde edilen geri dönme kaybı ve ışınım desenleri ölçüm sonuçları ile uyumlu çıkmıştır.

Anahtar Kelimeler: basılı çembersel monopol anten, yönsüz anten, düşük çapraz polarizasyonlu geniş bantlı anten, söndürmeli monopol anten, yüksek kazançlı monopol anten

ACKNOWLEDGEMENTS

I would like to thank Prof. Dr. Özlem Aydın Çivi, Prof. Dr. Sencer Koç, and Assoc. Prof. Dr. Lale Alatan for their support, supervision and understanding during the development of this thesis study. They always encouraged me with their fruitful advices and discussions.

I would like to thank Damla Alptekin, Aslı Eda Aydemir, Adem Ateş, Mehmet Ali Öztürk, Efecan Bozulu and Emre Alp Miran for their support and friendship through my thesis work.

TABLE OF CONTENTS

LIST OF TABLES

LIST OF FIGURES

LIST OF ABBREVIATIONS

BW	Bandwidth
HFSS	High Frequency Structure Simulator
(Field Computations	Involving Bodies of Arbitrary Shape)
FEM	Finite Element Method
MMIC	Monolithic microwave integrated circuit
NA	Not Available
VSWR	Voltage Standing Wave Ratio
UWB	Ultra-Wideband
LPKF	Leiterplatten Kopier Fræsen (Circuit board copy milling)

CHAPTER 1

INTRODUCTION

Wireless communication devices are becoming very popular for applications that use ultra-wide band (UWB) antennas such as video and data communication, airborne based RADAR, ground penetrating radar, UWB imaging etc. In 2002, Federal Communications Commission (FCC) announced 3.1 - 10.6 GHz bandwidth as UWB spectrum bandwidth for commercial applications. UWB antennas have low power consumption, high gain, simple structure, and low cost [3].

Through the years, microstrip patch antenna structures have become the most common option used for microwave, radar and communication applications. Microstrip antennas are very convenient for applications in wireless communication systems. However, a conventional microstrip antenna is limited because of poor gain, narrow bandwidth and polarization purity. For this reason, monopole antennas are gaining priority for handheld devices in the arena of UWB applications [1].

In recent years, several planar monopole antenna structures like circular, square, rectangular, elliptical have been proposed for UWB applications [3]. These monopole antenna geometries yield large impedance bandwidth. However, in these monopole antennas, patch and ground plane are perpendicular to each other, which increases the antenna volume. Moreover, planar antenna structures are very inconvenient for integration with microwave circuits. For these reason, planar monopole antennas are not suitable for microwave circuits. Printed monopole antennas are a better alternative for UWB communications.

In this study, UWB circular monopole antennas with omnidirectional radiation and low cross polarization characteristics are proposed. Furthermore, an UWB monopole antenna with band-notched performance is designed. Parametric studies are used to obtain large impedance bandwidth and low cross polarization. All of the designed antennas are fabricated. Simulated and measured return loss and radiation characteristics are compared to validate the designs. The bandwidth and size of the proposed antennas are compared with the previous designs available in the literature. A ring monopole antenna is designed and the ground plane is modified to reduce cross polarization and provide ultra-wide bandwidth. The UWB ring monopole antenna provides measured impedance bandwidth from 2.6 to over 20 GHz. An UWB antenna with symmetrically open-circuited stubs is designed. Parametric analysis is carried out in the symmetrical open circuited stubs in order to improve the radiation patterns of the antenna at high frequencies. The UWB antenna with symmetrically open-circuited stubs provides measured impedance bandwidths of 4.3-11.2 GHz. Moreover, an UWB antenna with band-notched characteristics (5-6.1 GHz) and with an omnidirectional radiation pattern is designed. U shaped slot is etched on the feedline to obtain band notched characteristics. The UWB band notched monopole antenna provides measured impedance bandwidth of 2.5-16.5 GHz.

This study provides performance comparison of omnidirectional, UWB circular monopole antennas based on radiation pattern, bandwidth, return loss, VSWR and gain. In antenna design, HFSS [2] (High Frequency Structure Simulator) is used as 3D electromagnetic field simulator, based on the FEM (Finite Element Method). Simulated and measured results which are presented in Chapter 5 found to be consistent with each other.

The surface current distribution of the antennas is analyzed using HFSS to explain the UWB radiation mechanism of the antenna.

The proposed designs are suitable for Hiper LAN 3.6 GHz (3657.50–3690.0 MHz) and IEEE 802.11 4.9-5.0 GHz (4915–5825 MHz), Bluetooth 3.30 GHz,

3.50 GHz (3400–3600 MHz) and 5.80 GHz (5.60–5.90 GHz) and LTE applications.

The chapters of the thesis are constructed as follows:

In Chapter 2, a literature review is given for UWB monopole antennas, omnidirectional monopole antennas, and radiation pattern improvements in monopole antennas.

In Chapter 3, simple circular monopole antenna is designed using parametric analyses. At the end of this study, design guidelines are prepared for simple circular monopole antenna.

In Chapter 4, the proposed antenna structures are explained. Return loss comparison, radiation patterns comparison and current distribution of the antennas are described by using parametric analyses.

In Chapter 5, simulated and measured results are presented and compared.

In Chapter 6, thesis study is summarized and obtained results are discussed.

CHAPTER 2

LITERATURE REVIEW

2.1 Introduction

Ultra-wideband antennas are very popular in wireless communication systems because of two main features. First, in both industry and academia, there is an increasing market for wideband antennas. Second, since the wireless portable devices operate in various frequencies, it is essential to manufacture small antennas with large bandwidth instead of using many antennas for many applications [3].

The bandwidth of an antenna is defined as "the range of frequencies within which the performance of the antenna, with respect to some characteristics, conforms to a specific standard in IEEE". The impedance bandwidth is the band of frequencies with VSWR less than 2. The fractional bandwidth and bandwidth ratio are also the most commonly used definitions for the antenna bandwidth. The fractional bandwidth is defined as

$BW_{fractional} = \frac{f_h - f_L}{f_c} x100\%$. [3]

The bandwidth ratio is defined as ratio of higher frequency to lower frequency [3] and it is expressed as

$BW = \frac{f_h}{f_L}$,

where f_h is the higher frequency of the operation band, f_L is the lower frequency of the operation band, and f_c is the center frequency of the operation band.

The radiation pattern bandwidth can be defined as “omnidirectional radiation gain which does not change more than 3 dB in the operating frequency band”.

In order to design UWB monopole antenna, it is crucial to have prior knowledge of UWB antenna techniques. Since this study focuses on printed UWB monopole antennas, some of the UWB monopole antennas are introduced in this chapter. The planar and printed monopole antennas are described and compared.

2.2 UWB Planar Monopole Antennas

Because of their wideband property, several planar monopole antenna structures are introduced in the literature [3]. Some of these antenna geometries and their bandwidth are given in Figure 1. These monopole antennas have bandwidth ratios up to 22.8:1.

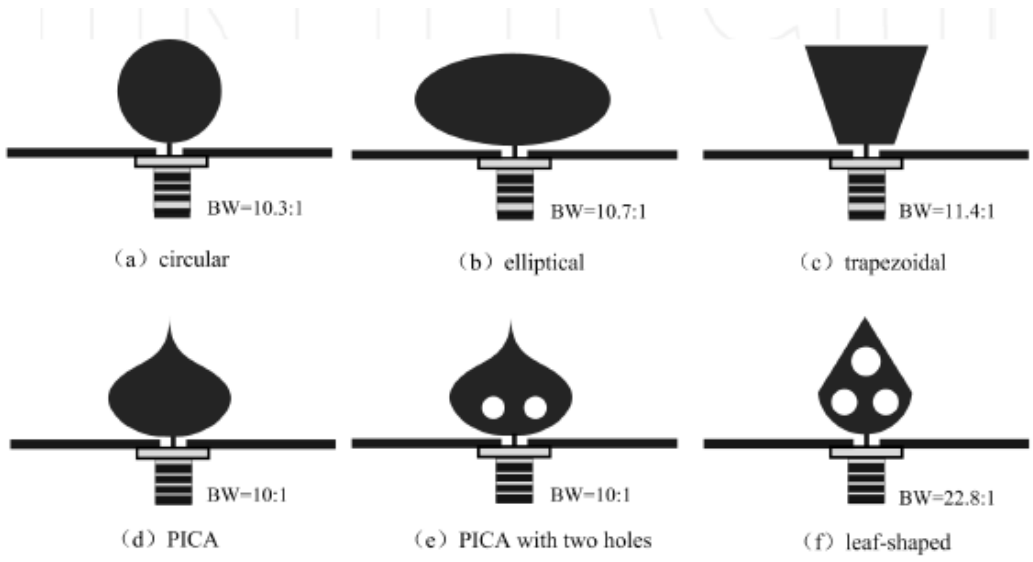

Figure 1: Planar monopole antennas with different geometries [3].

Impedance bandwidth ratio up to 10:1 can be achieved by circular and elliptical antennas (Circular planar monopole: 1.17-12 GHz, Elliptical planar monopole:

1.21-13 GHz). The planar inverted cone antenna (PICA) can yield bandwidth ratio up to 10:1, and its radiation pattern is better compared to circular monopole antenna [5]. PICA antenna geometry is obtained by trimming the top part of the circular disc. PICA antenna with two circular holes shown in Fig 1 (e) has the same impedance bandwidth ratio with PICA antenna. However, two circular holes in PICA antenna improve the radiation pattern by changing the current distribution on the antenna structure. The PICA antennas have omnidirectional radiation pattern bandwidth of 4:1, whereas PICA antennas with two circular holes have omnidirectional radiation pattern bandwidth of 8:1 [4].

One of the simplest geometry between different planar monopole antennas is square planar monopole antenna. Its radiation pattern does not change greatly in impedance bandwidth. However, it has narrow bandwidth. For this reason, some techniques are used to improve impedance bandwidth of the square planar monopole antenna [3].

Referring to Figure 2, various wideband techniques can be applied to planar square monopole.

1. The impedance bandwidth can be increased by opening rectangular slots in the bottom edge of the patch. The impedance bandwidth can be improved from 2.0-4.5 GHz to 2.0-12.7 GHz.
2. The double feed method increases impedance bandwidth ratio up to 9.5:1 [3]. Moreover, it increases the vertical current and decreases the horizontal current on antenna, which results in low cross polarization.
3. A trident-shaped feeding is used in order to avoid using two different feeding points as in the double feed method. Through this method, impedance bandwidth can be improved from 1.5-3.3 GHz to 1.4-11.4 GHz.

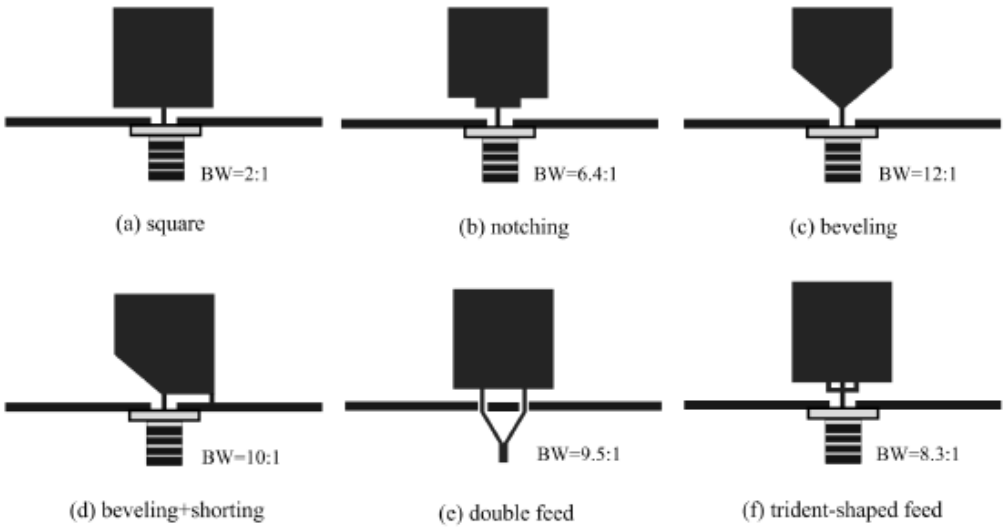

Figure 2: Different wideband methods for square planar monopole antennas [3].

2.3 UWB Printed Monopoles

The planar monopole antennas have wide bandwidth. However, in these antennas ground plane and patch are perpendicular, which makes them hard to use in microwave circuits. The printed UWB monopole antennas are more suitable for use in wireless communication. The ground plane and patch are both built in the same or opposite side of the substrate in printed monopole antennas.

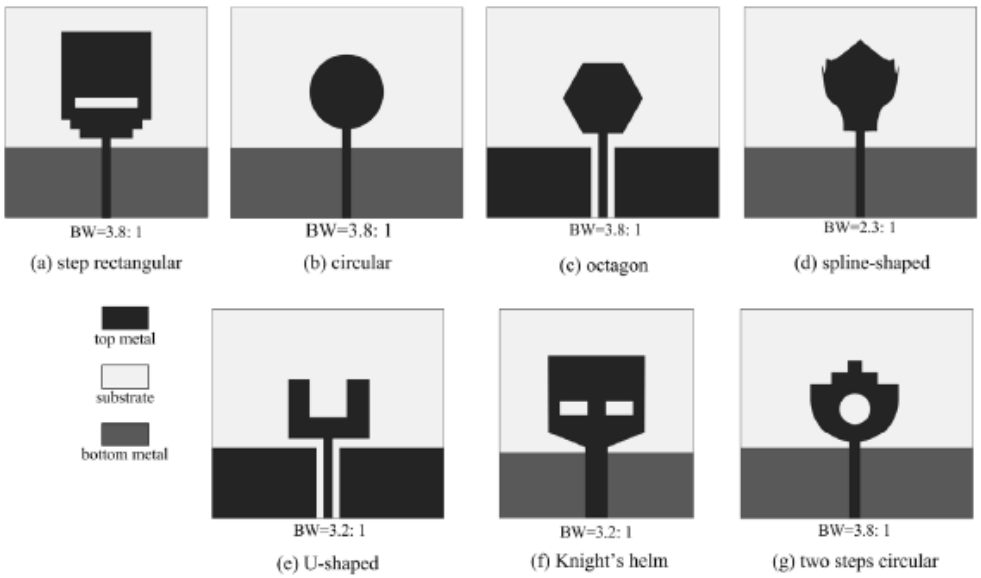

Figure 3: Different printed monopole antenna geometries [3].

Figure 3 presents several printed monopole geometries. Printed circular monopole antennas and other circular shape antennas provide impedance bandwidth ratio up to 3.8:1 [3].

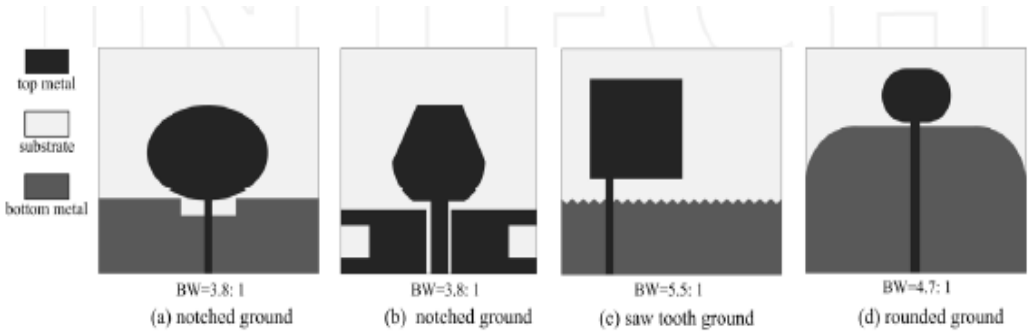

Figure 4: Different ground geometries for monopole antennas [3].

The geometry of the ground plane also affects impedance bandwidth. Various geometries for ground plane are shown in Figure 4. Opening rectangular slots on the top of the ground can increase impedance bandwidth (Figure 4.b) [3]. Moreover, saw tooth ground plane can yield impedance bandwidth ratio up to 5.5:1 (Figure 4.c). A rounded truncated structure (Figure 4.d) at ground plane also provides impedance bandwidth ratio up to 4.7:1 [3].

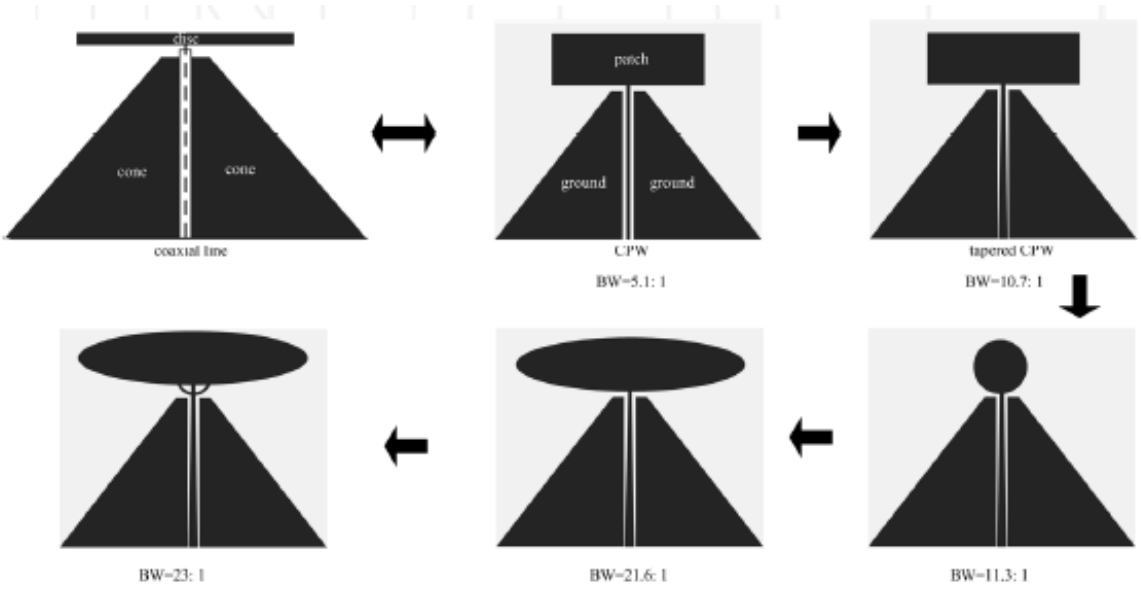

Figure 5: Different monopole antennas with trapeziform shaped ground [3].

Trapeziform shaped ground plane is also used in some antennas in the literature to obtain large bandwidth as shown in Figure 5 [3].

In this thesis study, printed circular monopole is considered as the basic element and some of the techniques mentioned in this section are applied to improve antenna characteristics. First, simple circular monopole antenna is designed. A small rectangular slot is etched on the ground plane in order to enhance bandwidth. Chamfer edged ground plane is used in this study for bandwidth enhancement. In order to improve radiation pattern, rectangular slots are etched on the ground plane. Moreover, circular hole in the patch is used for both bandwidth enhancement and radiation pattern improvement. The designed UWB Ring Monopole antenna provides omnidirectional pattern over simulated wideband 8.3:1 and measured 5.5:1. Also, symmetrically parallel open circuited stubs are used to improve radiation pattern at high frequencies.

There are many narrow band communication frequencies inside FCC's licensed band and they produce interferences with UWB communication band. Building stopband filter inside antenna structure can prevent these interferences, and the size of the system can be minimized [16].

Some band-notched antennas which have notches on the ground plane and patch are proposed in the literature [15-16]. However, these antennas have narrow bandwidth. A UWB antenna with WLAN (5 GHz–6.1 GHz) band notched performance is designed and analyzed in this thesis. This proposed monopole antenna has larger bandwidth with respect to the reference antennas in [13-14] and this antenna can easily be used with many communication devices.

CHAPTER 3

DESIGN OF SIMPLE CIRCULAR MONOPOLE ANTENNA

3.1 Design of Simple Circular Monopole Antenna

Simple circular monopole antennas are known as a good candidate for UWB applications since they have wideband characteristics, simple geometry, simple manufacturing, and omnidirectional pattern.

A simple circular monopole antenna structure is shown in Figure 6. It is a circular patch of radius *r* on a dielectric substrate of thickness *h*. There is a partial ground plane behind the patch. The patch is fed by 50 Ω microstrip line.

The size of the circular disc defines lower frequency of the simple circular monopole antenna [5]. Wide frequency band is associated with the number of modes that resonate.

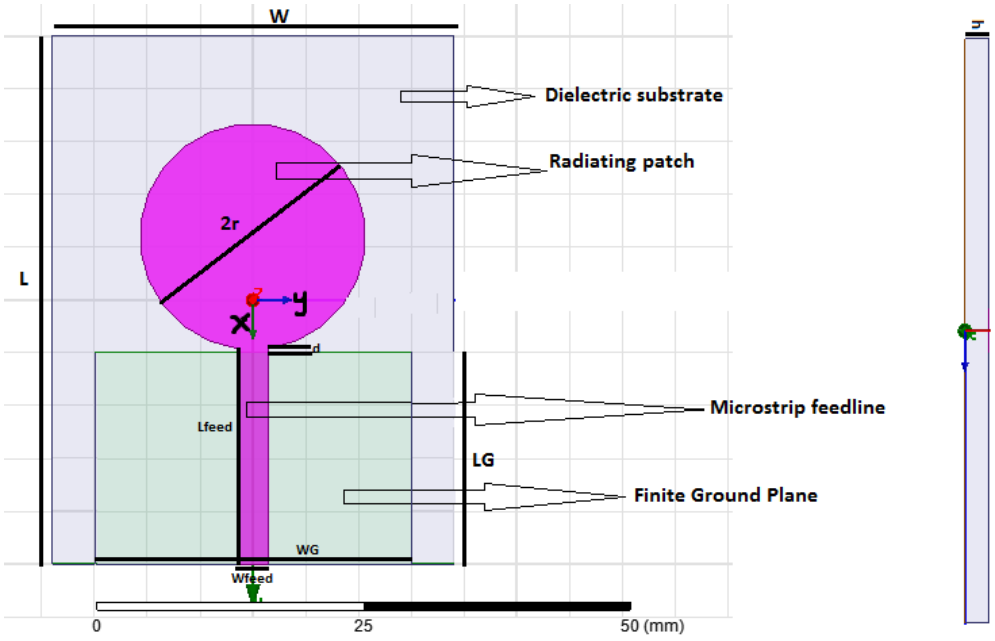

Figure 6: Geometry of the simple circular monopole antenna.

Initial design parameters can be calculated from the formulas given in [6]. For the intended lower frequency of 3.1 GHz, the radius is calculated from

$$f_L = \frac{7.2}{2.25r+d} \ ,$$

where f_L is the lowest resonance frequency in GHz, r is the radius of circular patch in cm, and d is the gap between monopole patch and ground plane in cm. At 3.1 GHz for d=0, radius is calculated as 10.7 mm. The antenna is printed on FR4 epoxy ($\varepsilon = 4.4$) with thickness (h) of 1.6 mm, and loss tangent of 0.02.

The substrate length is chosen as half wavelength of the lowest frequency. The antenna substrate width is 42 mm and length is 50 mm in this design.

The feeding line width is calculated by using the transmission line theory. Figure 7 shows geometry of a transmission line. The approximated relative permittivity is given in [7] as

$$\varepsilon_{re} = \frac{\varepsilon_r+1}{2} + \frac{\varepsilon_r-1}{2\sqrt{1+12h/W_{feed}}} ,$$

where h is the thickness of the substrate in this formula. For W_{feed}/h <1, the line characteristic impedance is given as

$$Z_0 = \frac{60}{\sqrt{\varepsilon_r}} In\left(\frac{8h}{W_{feed}} + \frac{W_{feed}}{4h}\right) > \frac{126}{\sqrt{\varepsilon_r}} \ .$$

For W_{feed}/h >1, the impedance of the line is

$$Z_0 = \frac{120\pi}{\sqrt{\varepsilon_r}\left(\frac{W_{feed}}{h}+1.393+0.667In\left[\frac{W_{feed}}{h}+1.44\right]\right)} < \frac{126}{\sqrt{\varepsilon_r}} \ ,$$

where *In* is the natural logarithm, which has base e.

It is seen that, as W_{feed}/h ratio or permittivity increases, impedance decreases. By using this formula and the initial antenna parameters given above (permittivity of 4.4 and thickness of 1.6mm), the feedline width is calculated. After this calculation, $Z_0 = 50\ \Omega$ is achieved when $W_{feed} = 2.85\ mm$.

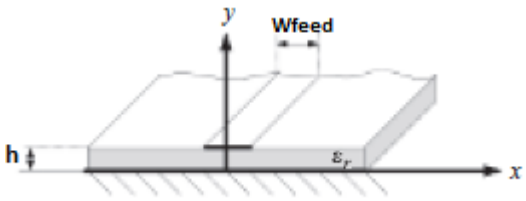

Figure 7: Microstrip line [7].

Antenna with the calculated dimensions is simulated by HFSS. The gap (*d)* between monopole patch and ground plane, width of ground plane (W_g), length of the ground plane (L_g) affect impedance bandwidth of monopole antenna. This is because the current distribution is at the edges of the monopole patch and on the upper edges of the ground plane.

Dimensions of the designed antenna are given in Table 1.

Table 1: Simple circular monopole antenna parameters

Dimension	Unit (mm)	Dimension	Unit (mm)
L	50	W_{feed}	2.85
W	42	L_g	20
r	10.7	W_g	42
d	0.4	h	1.6
ε	4.4		

The return loss of the antenna as a function of frequency is plotted in Figure 8. The 10 dB bandwidth of the antenna is 2.5 -10.4 GHz.

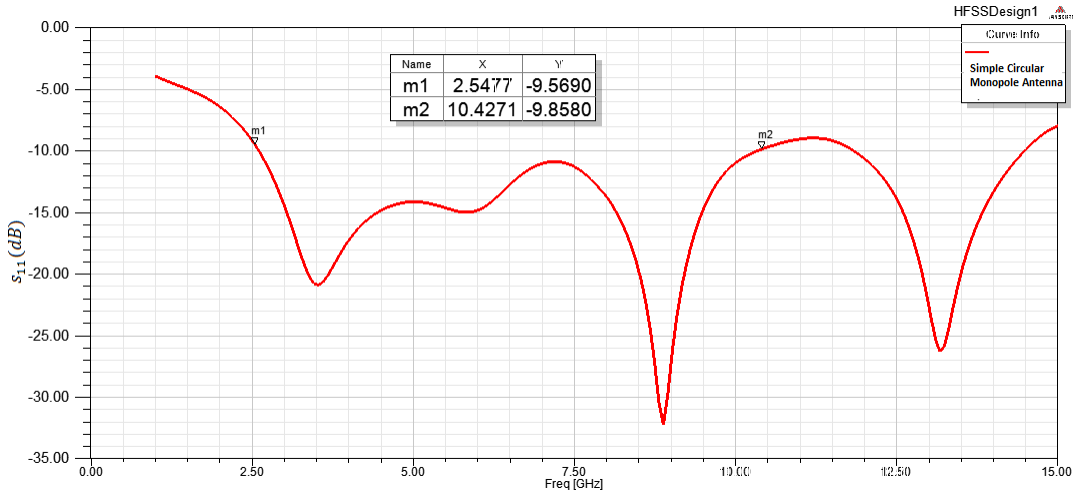

Figure 8: S_{11} versus frequency for optimized antenna.

The current distribution of the simple circular monopole antenna at frequencies of 3, 6, 9 and 13 GHz is shown in Figure 9 and Figure 10.

The current on the antenna shows that larger part of the current is distributed along the edge of the circular patch and upper edge of ground plane. On the patch, one half-cycle of current variation is observed, which indicates the fundamental mode of the antenna at 3 GHz. The current distribution at 6 GHz has two half-cycle of current variations on the patch. The current distribution at 9 GHz has three half-cycle of current variations as that at 3 GHz on the patch. At 13 GHz, strong currents are observed on the ground plane. Existence of strong currents on the ground plane indicates that ground plane dimensions have effect on bandwidth of the antenna.

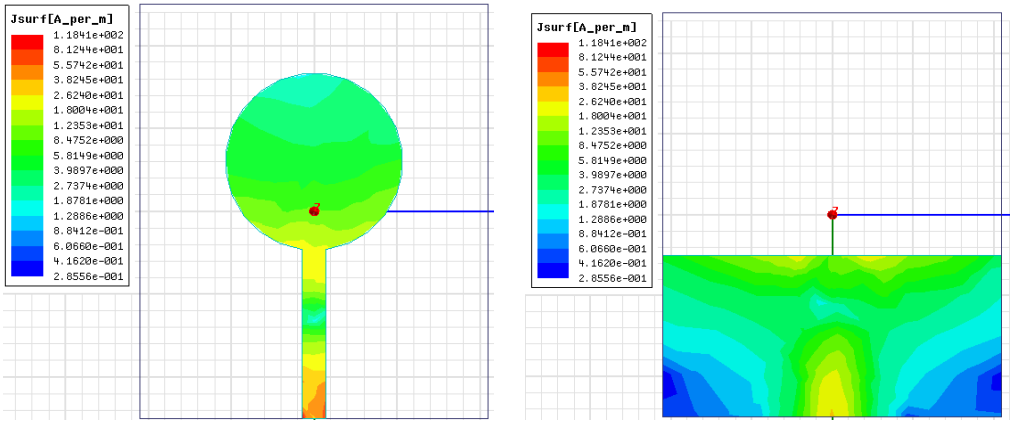

(a) 3 GHz

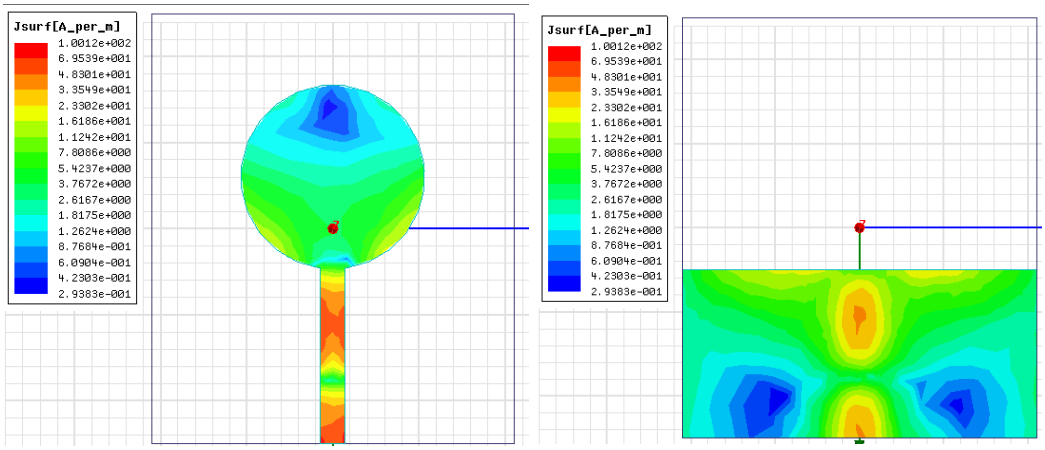

(b) 6 GHz

Figure 9: Simulated current distributions of antenna at 3 GHz, 6 GHz.

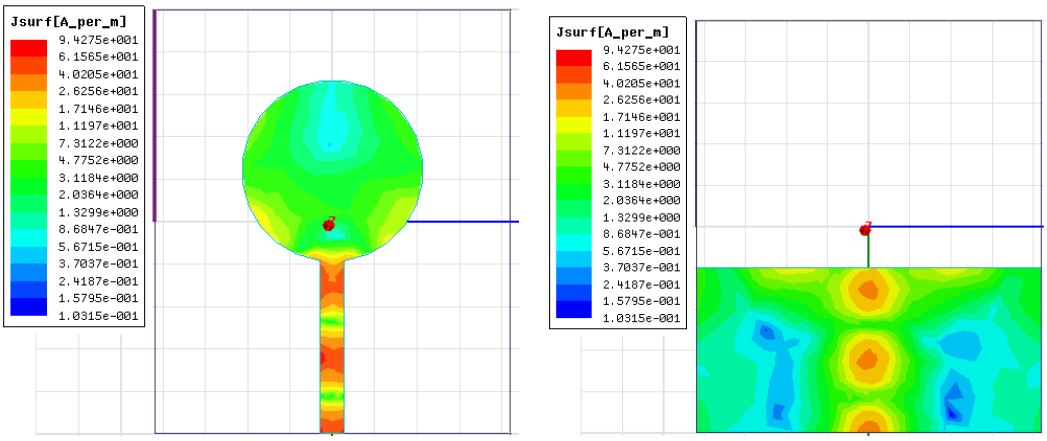

(c) 9 GHz

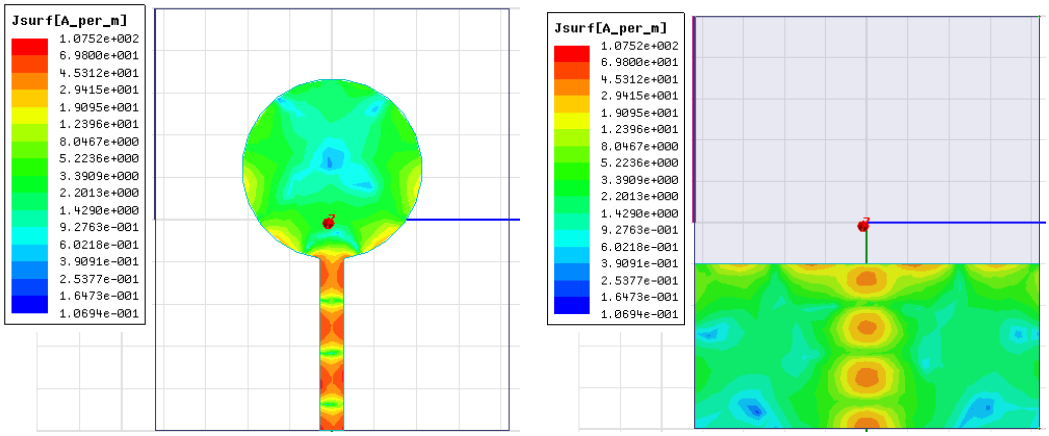

(d) 13 GHz

Figure 10: Simulated current distributions of antenna at 9 GHz and 13 GHz.

In order to understand the effect of each parameter on the performance of the antenna, parametric analysis is carried out and presented in Chapter 2.

3.2 Parametric Study of Simple Circular Monopole Antenna

Simulations are performed using the HFSS simulation package in order to reveal how antenna parameters affect antenna bandwidth. Following this study, design guidelines are proposed for simple circular monopole antenna.

The effect of different parameters, such as the gap (*d)* between monopole patch and ground plane, width of ground plane (W_g), length of the ground plane (L_g), dielectric constant (ε), thickness (*h*), and patch radius (*r*) are studied [8-9].

3.2.1 Effect of the width of ground plane (Wg)

Ground plane width affects the impedance bandwidth of the antenna. In this part of the study, only width of ground plane (W_g) is changed, while substrate width is fixed as 42 mm. The other parameters of the antenna remain fixed. For ground plane widths of 30 mm, 36 mm, 42 mm, Figure 11 shows s_{11} versus frequency.

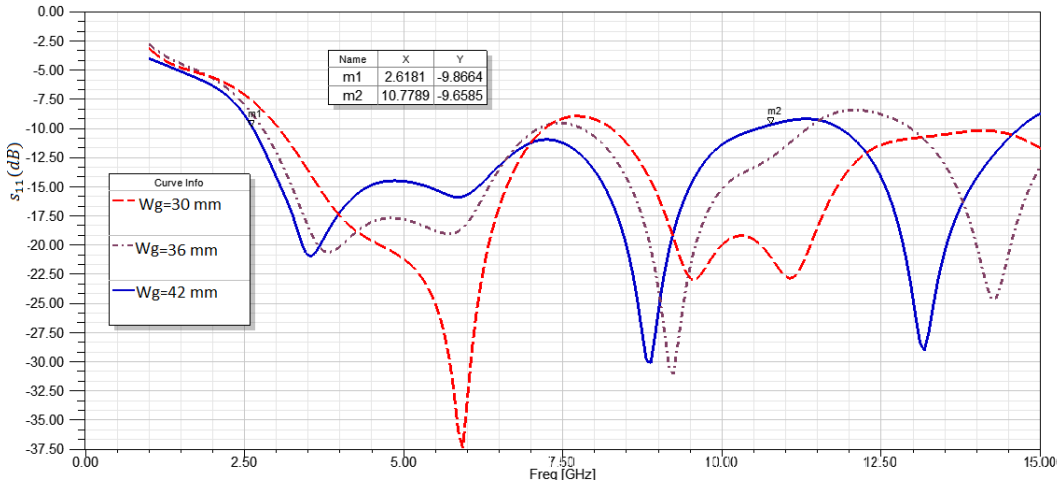

Figure 11: s_{11} versus frequency for various ground plane widths.

It is seen that as W_g changes, the second resonant frequency does not change very much but the first and third resonant frequency behavior changes significantly. The resonant frequencies also shift down with increase in ground plane width.

Moreover, for the dimensions of W_g=30 mm and W_g=36 mm, it is observed that bandwidth is smaller. The antenna gives widest impedance bandwidth ($|s_{11}|$<-10 dB) when W_g=*42* mm. It is seen that the antenna gives the widest impedance bandwidth when ground plane and substrate have the same width.

3.2.2 Effect of the length of the ground plane (*Lg*)

In this part, a parametric analysis is used to see the effect of ground plane length in bandwidth. Only length of ground plane (L_g) is changed. The other parameters of the antenna remain fixed.

Return loss is plotted as a function of frequency in Figure 12 for ground plane lengths of 8 mm, 12 mm, 16 mm, 20 mm, 22 mm and 24 mm. It is seen that there is not a significant effect of L_g in bandwidth enhancement.

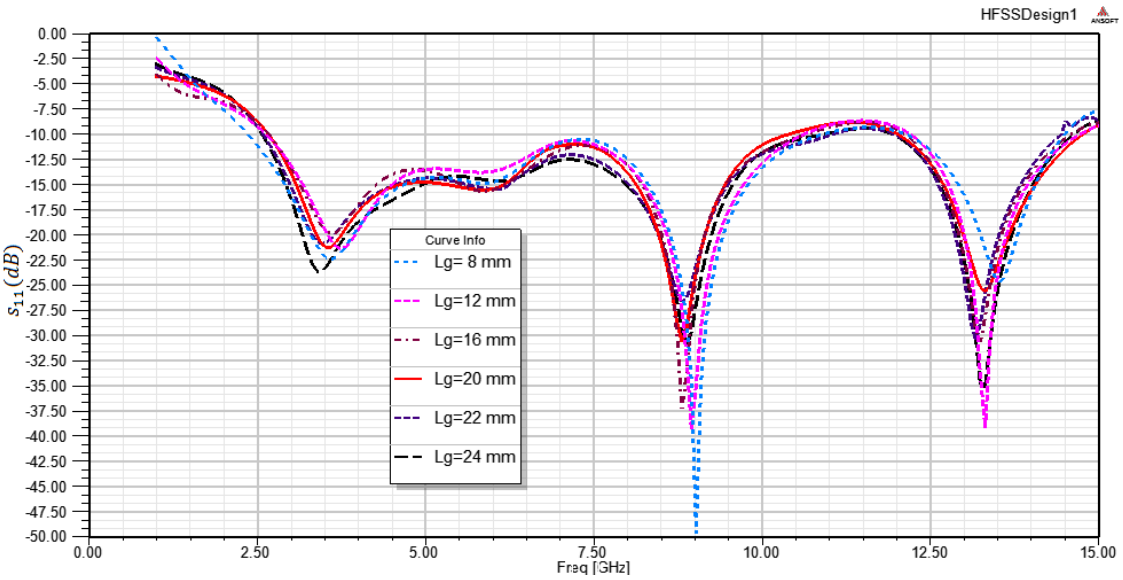

Figure 12: s_{11} versus frequency for various ground plane lengths.

Resonant frequencies shift down slightly with increase of the parameter L_g.

3.2.3 Effect of the dielectric constant (ε)

In this part of the study, the effect of dielectric constant on bandwidth is observed. The antenna is simulated with FR4 epoxy ($\varepsilon = 4.4$), RT 4003 ($\varepsilon = 3.55$) and RT 5880 ($\varepsilon = 2.2$). The microstrip feed line width is varied accordingly such that the characteristic impedance remains 50 Ω. Table 2 shows the width of the 50 Ω microstrip feed line for varying dielectric materials. The width of the feed line varies from 2.85 mm to 4.92 mm.

Table 2: Width of 50 Ω microstrip feed line for different dielectric constants

$\boldsymbol{\varepsilon}$	4.4	3.55	2.2
$\boldsymbol{W_{feed}}$ **(mm)**	2.85	3.72	4.92

s_{11} versus frequency is plotted for various dielectric constants in Figure 13. As seen, dielectric constant changes impedance bandwidth of the antenna.

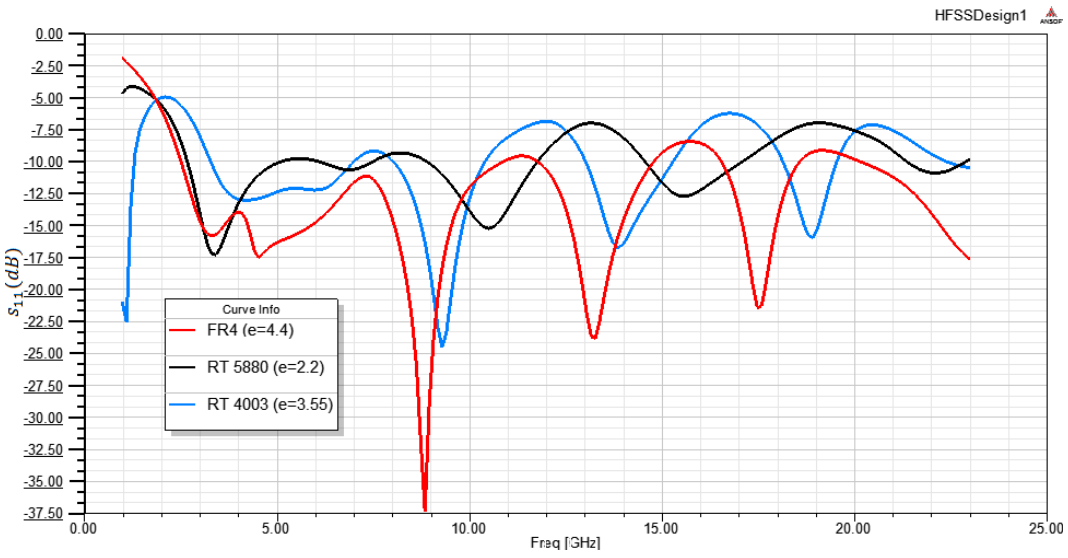

Figure 13: s_{11} versus frequency for various dielectric constants.

Four resonances are observed for FR4, whereas three resonances are observed for RT 5880 and RT 4003. Moreover, the resonances are shifted towards the lower frequency with the increase in dielectric constant.

Radiation pattern of antenna for FR4 and RT 5880 GHz is compared in Figure 14 at frequencies of 3, 6, 9 and 12. It can be seen that change in radiation pattern is more significant at high frequencies because change in resonances at high frequencies. The cross polarization component decreases slightly as dielectric constant decreases.

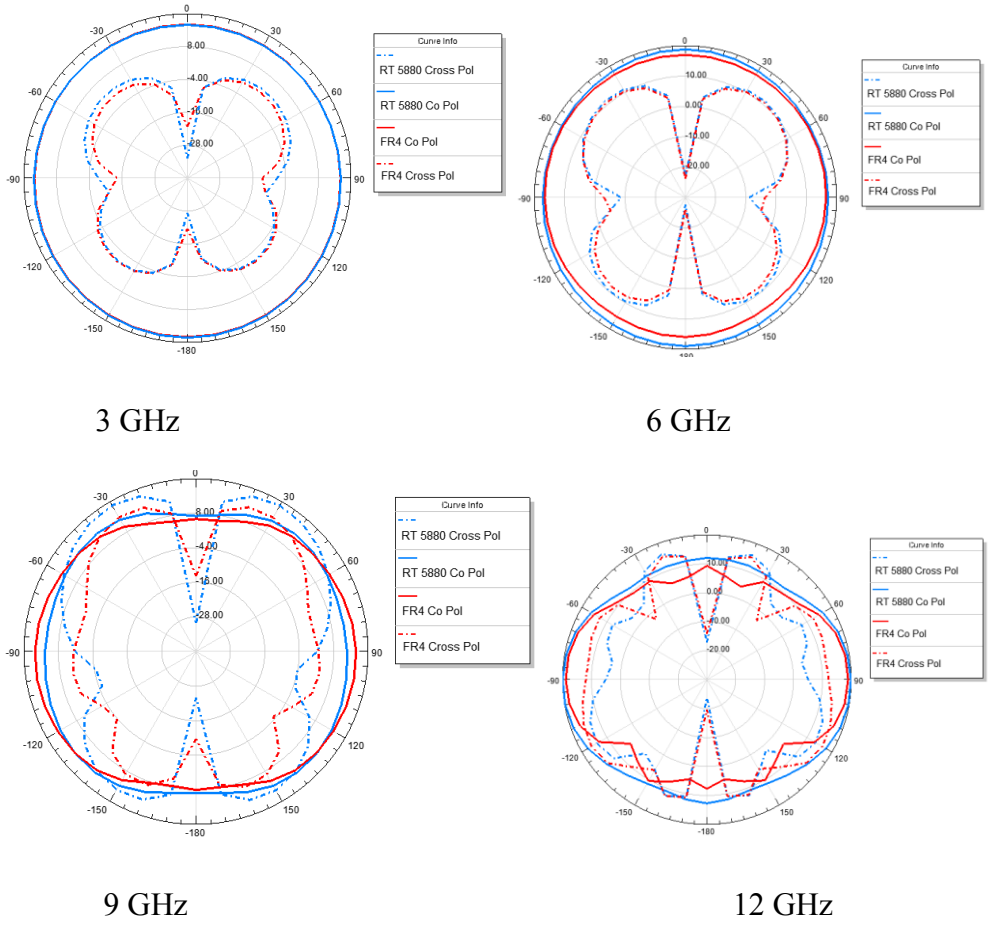

Figure 14: H(y-z) plane radiation pattern for different dielectric materials.

3.2.4 Effect of the thickness (*h*)

The substrate thickness also affects impedance bandwidth of antenna. To observe this effect, *h* is changed from 0.5 mm to 2 mm by 0.5 mm steps. The microstrip feed line width is varied accordingly such that the characteristic impedance of line remains 50 Ω. Other parameters of the antenna remain fixed.

Table 3 shows the width of the 50 Ω microstrip feed line for varying substrate thickness. The width of the feed line varies from 0.95 mm to 3.82 mm.

Table 3: Width of 50 Ω microstrip feed line or varying substrate thickness

h **(mm)**	0.5	1	1.5	2
W_{feed} **(mm)**	0.95	1.91	2.86	3.82

Figure 15 shows s_{11} versus frequency for thickness values of 0.5 mm, 1 mm, 1.5 mm, and 2 mm.

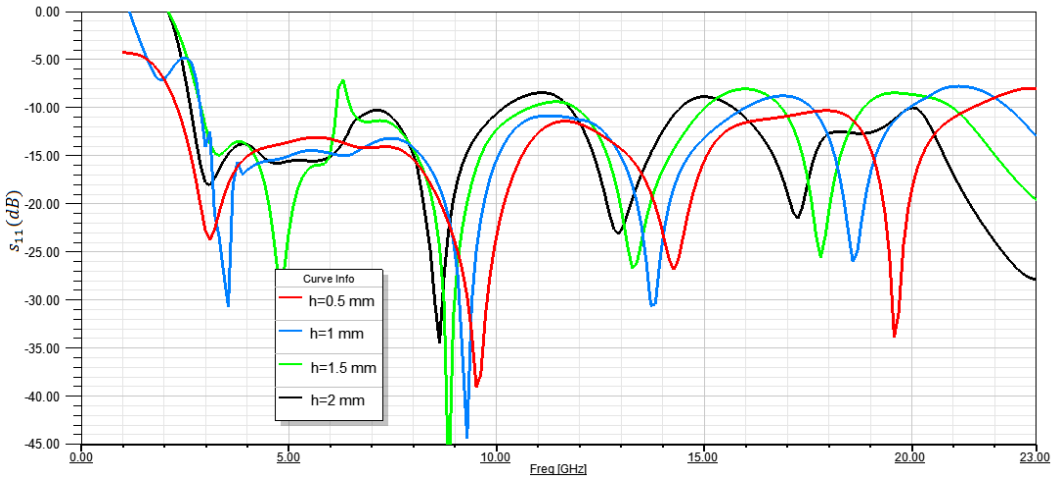

Figure 15: s_{11} versus frequency for various substrate thickness.

As seen, the first resonant frequency of the antenna has minimal variation. However, there is a significant effect of h in the second, third and fourth resonant

frequencies. The resonances are shifted towards the lower frequency with the increase in thickness.

Radiation pattern of antenna for substrate thickness values of 0.5 mm, and 2 mm at frequencies of 3, 6, 9 and 12 GHz is plotted in Figure 16. The effect of thickness on radiation pattern is more significant at high frequencies because resonant frequencies of antenna changes greatly at high frequencies. It can be seen that cross polarization component decreases as thickness value decreases.

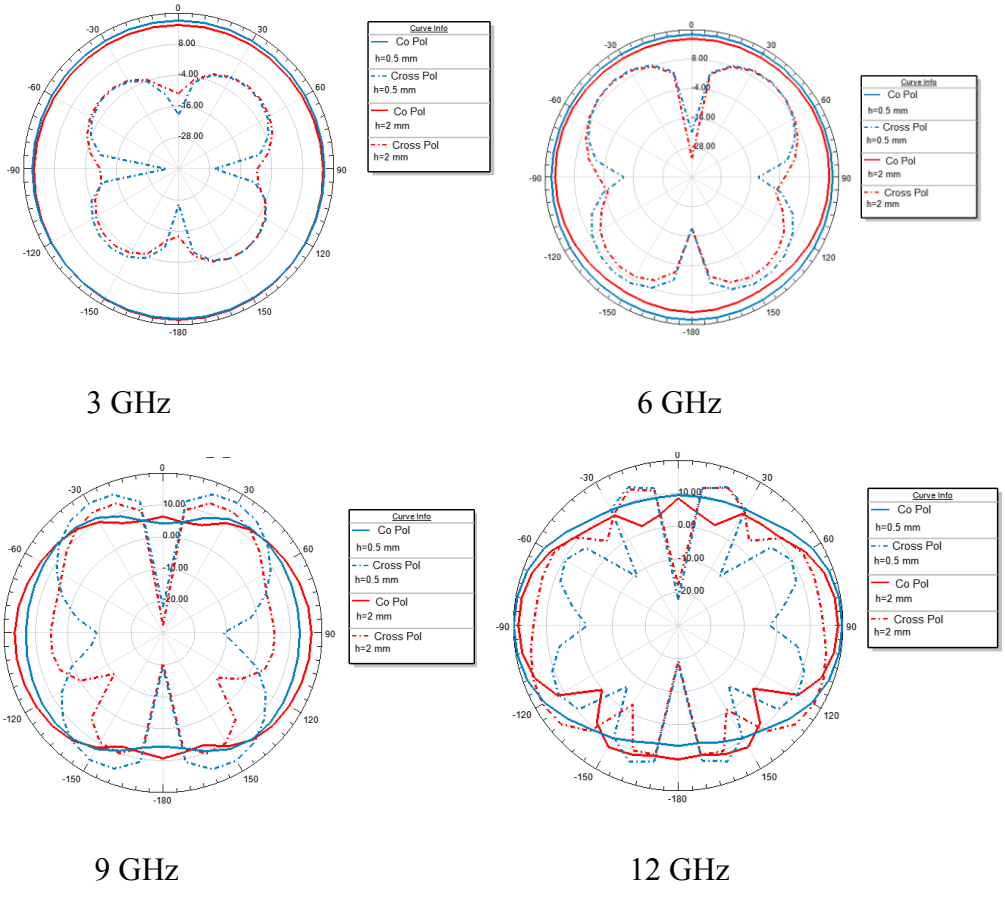

Figure 16: H(y-z) plane radiation pattern for various substrate thickness values.

3.2.5 Effect of the Gap between Monopole Patch and Ground Plane (d)

The gap (*d*) between monopole patch and ground plane affects the impedance bandwidth of the antenna. In this part of the study, only the gap (*d*) is changed. The other parameters of the antenna remain fixed. $|S_{11}|$ is plotted in Figure 17 for gap lengths of 0.4 mm, 1.2 mm, 2 mm, and 2.8 mm.

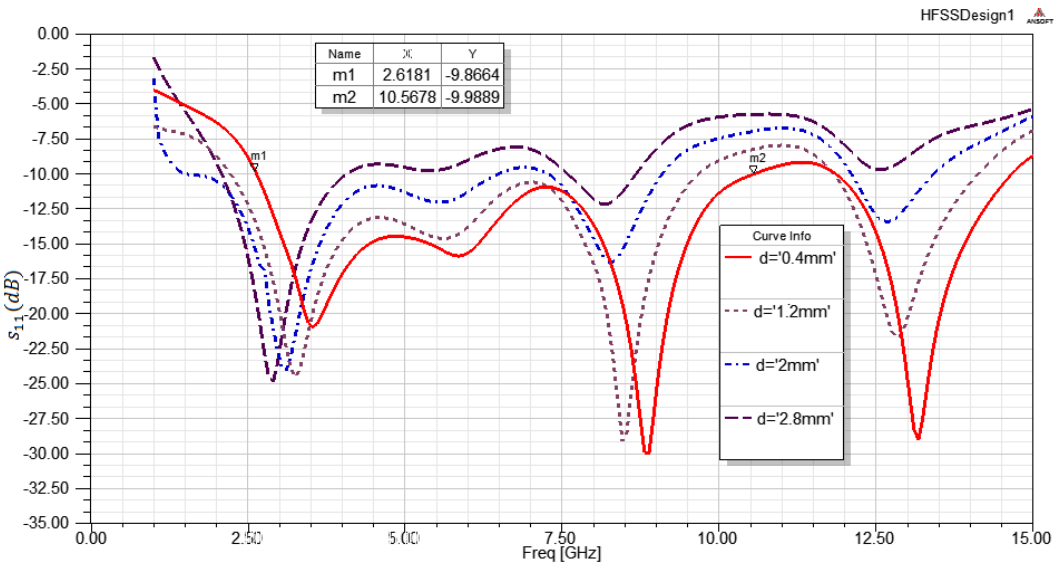

Figure 17: S_{11} versus frequency for different gap lengths (*d*).

It is seen that as *d* decreases, resonant frequencies shift to upper side. The first resonant frequency does not change very much but the second and third resonant frequency behavior change significantly. The change in second and third resonant frequency improves the antenna bandwidth.

As summary, the impedance matching is sensitive to the gap between patch and upper edge og ground plane.

3.2.6 Effect of Patch Radius (*r*)

The radius of the circular patch affects impedance bandwidth as well. Only the patch radius (*r*) is changed. The other parameters of the antenna remain fixed.

s_{11} versus frequency is plotted in Figure 18 for radii of 5.7 mm, 8.2 mm, 10.7 mm, and 13.2 mm. The first resonant frequency of the antenna is reduced with the increase in radius size. The radius of the patch determines the first resonance frequency.

When the radius of circular monopole is set as r = 10.7 mm, the antenna has widest bandwidth (2.6 GHz - 10.5 GHz) compared with the other radii.

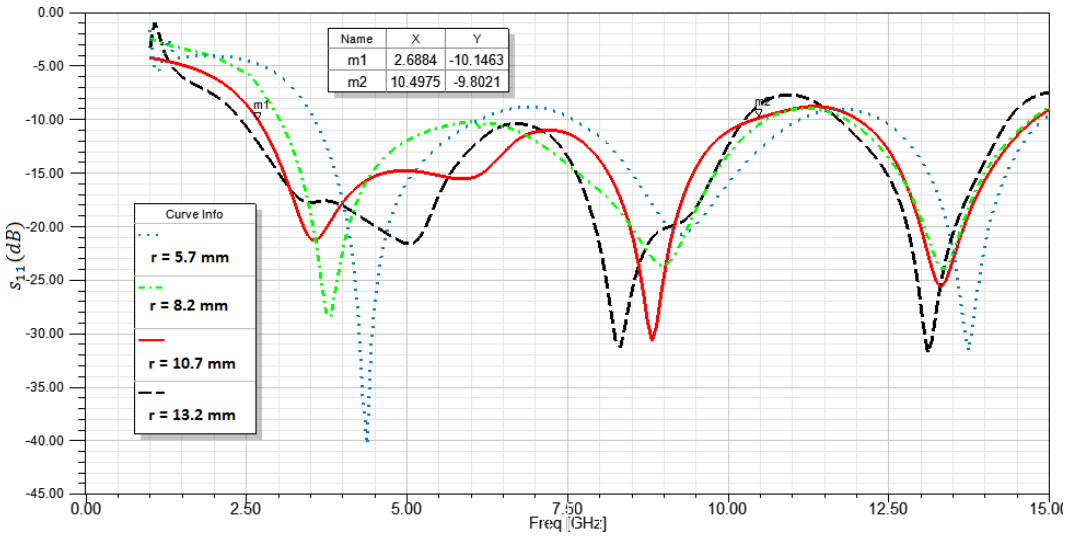

Figure 18: s_{11} versus frequency for different radii.

3.3 Design Guidelines for Simple Circular Monopole Antenna

The designed simple circular monopole antenna has an impedance bandwidth from 2.6 to 10.4 GHz. It is seen that, impedance bandwidth changes with the physical parameters of the antenna such as the gap (*d)* between monopole patch and ground plane, width of ground plane (W_g), length of the ground plane (L_g),

dielectric constant (ε), thickness (h), and patch radius (r). In order to design a simple circular monopole antenna, the following steps can be applied.

1. Define lower operating frequency of antenna and calculate patch radius (r) by using the formula f_L =7.2/(2.25r + d). If the radius size decreases, the lower frequency of antenna increases.

2. Calculate the width of the feeding line by using the transmission line theory.

3. Ground plane width (W_g) changes impedance bandwidth. An increase in ground plane width improves bandwidth of the antenna. It is seen that the antenna gives the widest impedance bandwidth when ground plane and substrate have the same width.

4. The length of the ground plane (L_g) also affects the return loss characteristics of the antenna. An increase in L_g improves impedance bandwidth of the antenna.

5. Dielectric constant (ε) changes impedance bandwidth of the antenna as well. The numbers of resonances increase with the increase of dielectric constant.

6. The substrate thickness (h) also affects impedance matching of antenna. The resonances are shifted towards the lower frequency with the increase in thickness.

7. It is observed that the gap (d) between lower edge of patch and upper edge of ground plane has a significant effect on impedance matching. As gap between ground plane and patch decreases, antenna impedance bandwidth increases.

3.4 Radiation Pattern of Simple Circular Monopole Antenna

Figure 19 and Figure 20 show simulated co and cross polarized fields in E (x-z) and H (y-z) planes at 3, 6 and 9 GHz. On the E plane, the antenna has near-omnidirectional pattern, and on the H plane, the antenna has omnidirectional pattern. However, at high frequencies, the omnidirectional characteristics of the antenna degrade. In operating frequency band, the cross-polarization level is below -15 dB in E plane but it is high on the H plane. It is anticipated that high cross polarized fields are due to horizontal currents on the upper edge of ground plane. Thus, it should be improved.

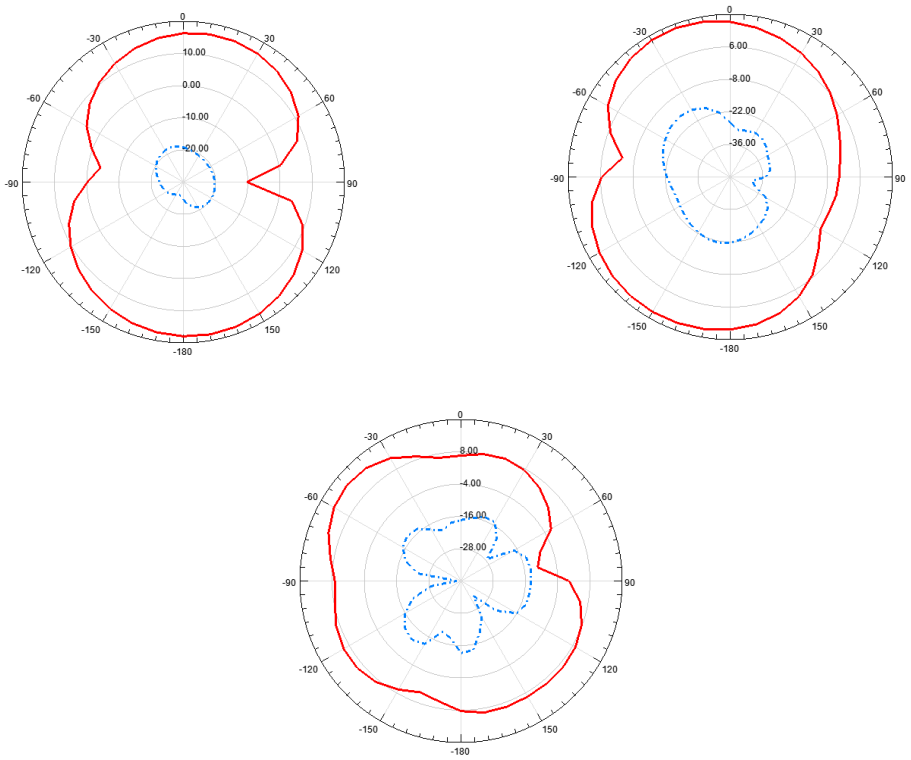

Figure 19: Simulated E plane patterns (co-pol: red, cross pol: dashdot-blue).

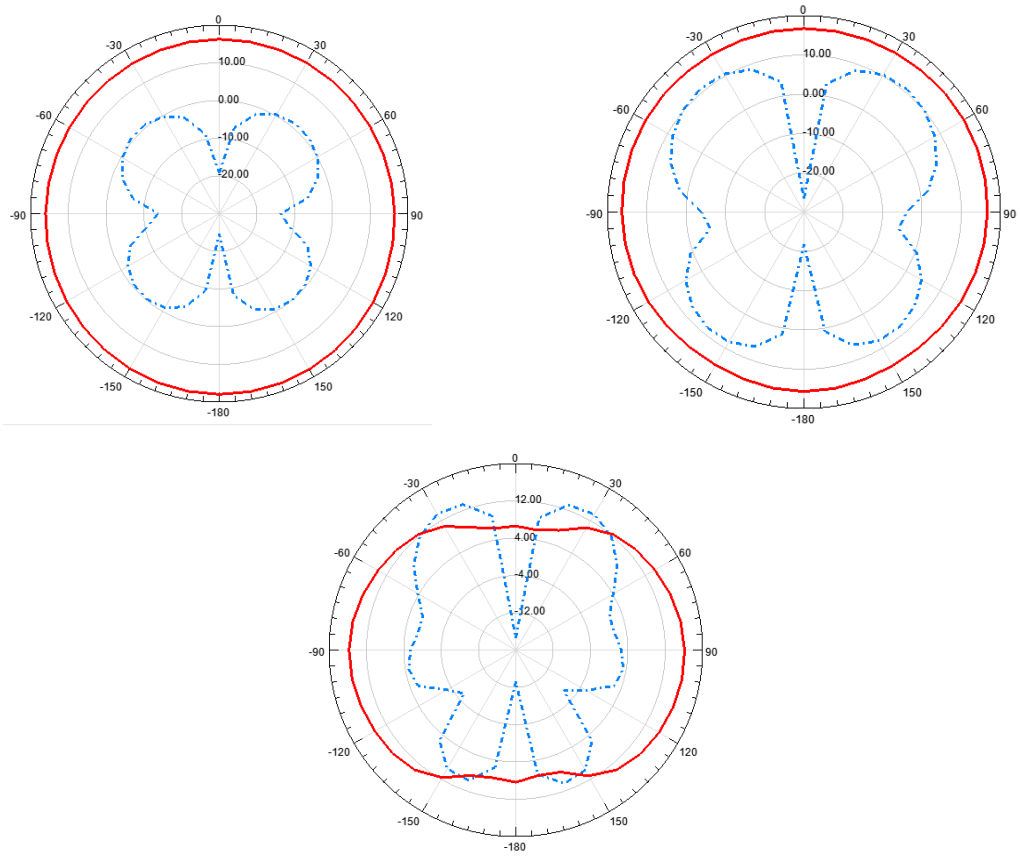

Figure 20: Simulated H plane patterns (co-pol: red, cross-pol: dashdot-blue).

Both impedance bandwidth and radiation pattern of the antenna can be improved by using some of the techniques given in Chapter 2. After using these techniques, bandwidth is extended, while cross polarization on the H plane is drastically reduced. In Chapter 4, proposed antennas will be introduced.

CHAPTER 4

DESIGN AND ANALYSIS OF THE PROPOSED CIRCULAR MONOPOLE ANTENNAS

In this chapter, the design and analysis of proposed antennas are presented.

4.1 Design of Ultra-Wideband Ring Monopole Antenna

This study proposes a microstrip line fed circular monopole antenna with ultra-wideband characteristics (3.0 GHz-21.3 GHz) and improved omnidirectional radiation pattern. All antennas are designed and produced on FR4 epoxy ($\varepsilon = 4.4$) with thickness of 1.6 mm and loss tangent of 0.02. The evolution of the antenna from the simple circular monopole antenna is shown in Figure 21.

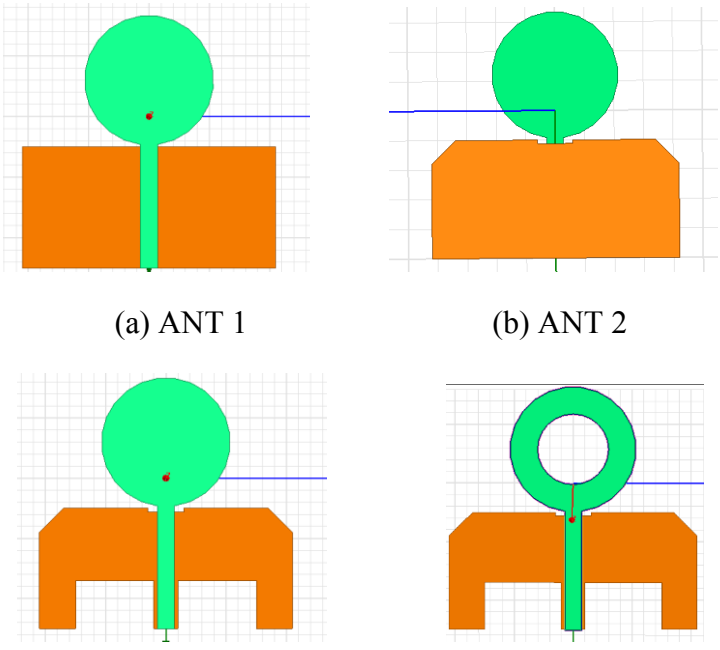

(a) ANT 1 (b) ANT 2

(c) ANT 3 (d) ANT 4

Figure 21: Design process of UWB ring monopole antenna.

The simple circular monopole antenna is modified to get ANT 2 in order to increase impedance bandwidth. In ANT 2, two corners of the upper edge of ground plane are tapered as 4 mm x 4 mm. Moreover, a small notch of 0.6 mm x 6 mm is embedded in the middle top of the ground plane as shown in Figure 22.

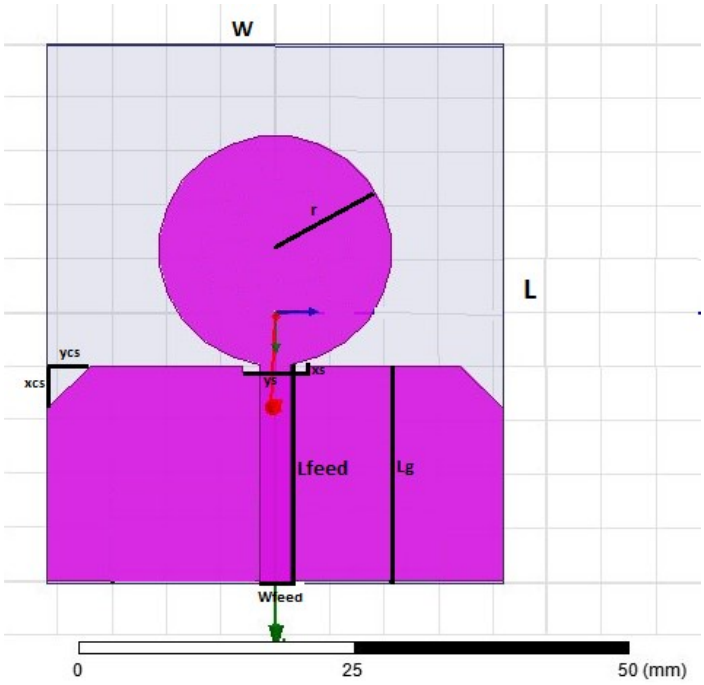

Figure 22: Geometry of ANT 2.

Antenna dimensions are found by using parametric analysis and are given in Table 4.

Table 4: ANT 2 Parameters

Dimension	Unit (mm)	Dimension	Unit (mm)
L	50	L_{feed}	20.4
W	42	L_g	20
r	10.7	x_s	0.6
x_{cs}	4	y_s	6
y_{cs}	4		

The simulated $|S_{11}|$ values for ANT 1 and ANT 2 are compared in Figure 23. ANT 1 bandwidth extends from 2.5 GHz to 10.4 GHz, while ANT 2 bandwidth extends from 2.5 GHz to over 21.8 GHz. The capacitive and inductive

characteristics of the antenna can be changed and impedance bandwidth can be enhanced by tapering corners and cutting a small notch of suitable dimensions on the ground plane.

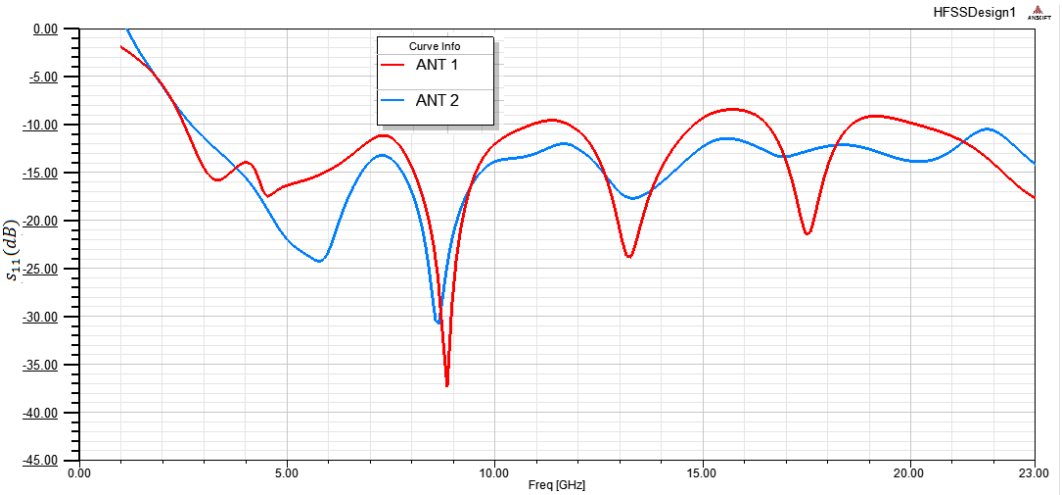

Figure 23: s_{11} versus frequency for ANT 1 and ANT 2.

Figure 24 shows simulated radiation patterns of ANT 1 and ANT 2 respectively at 3, 6, 9 GHz.

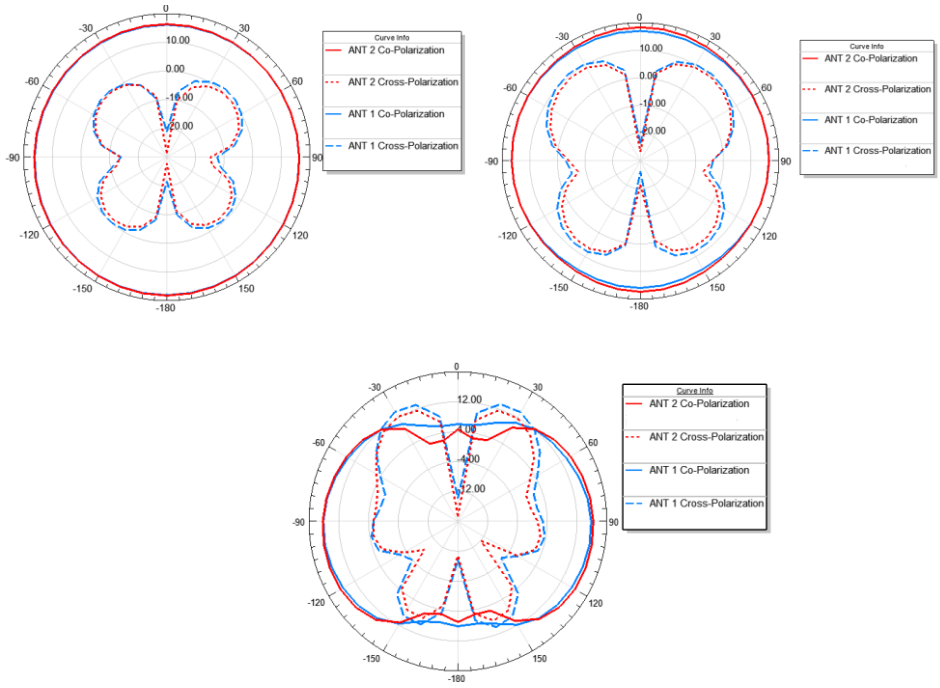

Figure 24: Simulated H (y-z) plane patterns of ANT 1 and ANT 2

As seen from Figure 24, ANT 1 and ANT 2 have almost the same radiation pattern in all frequencies.

Total current distribution of ANT 2 at 9 GHz is given in Figure 25. ANT 2 has high cross polarization at higher frequencies because of the excess amount of horizontal currents on the edge of the ground plane close to feedline.

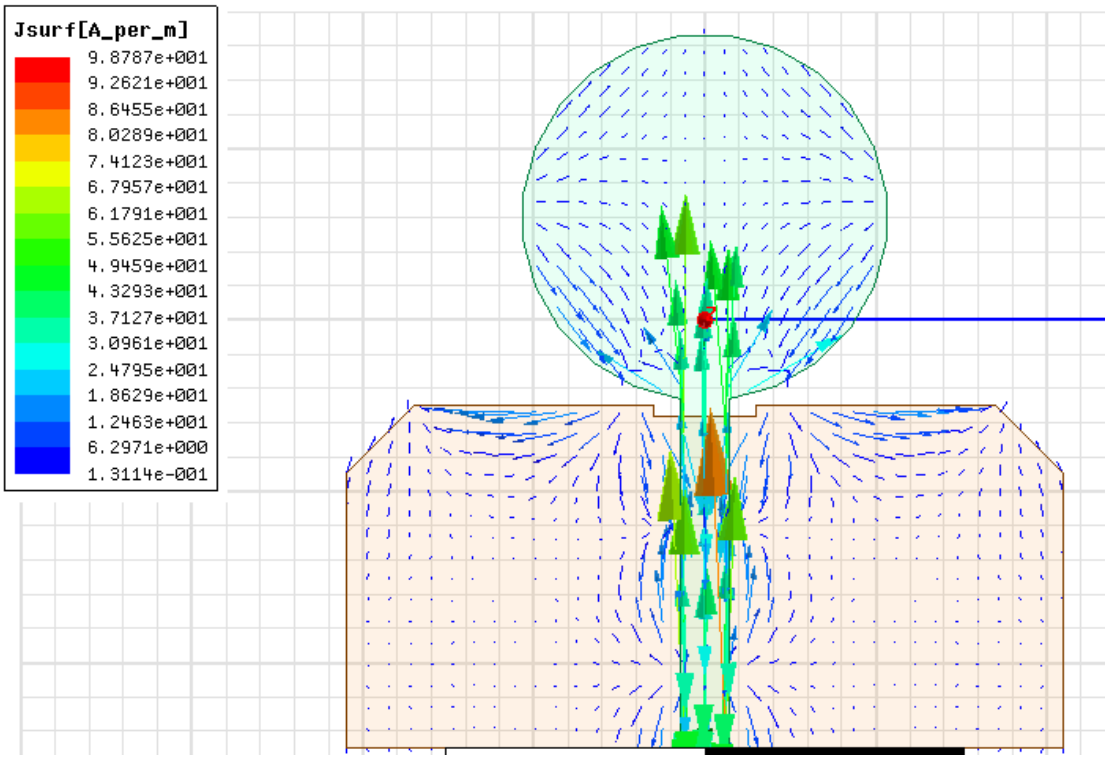

Figure 25: Total current at 9 GHz for ANT 2.

In order to improve radiation pattern in frequency band of designed antenna, ANT 2 is modified to get ANT 3 as shown in Figure 21.c. Two notches of suitable dimensions are cut on bottom of the ground plane to alter current flow paths.

Current distribution of the ANT 3 is plotted in Figure 26. It is seen that some of the currents are distributed on the edges of two rectangular notches (x_{gs}, y_{gs}), which decreases current density around the feedline. Moreover, the horizontal currents on upper and lower side of ground plane are in opposite direction. It is

anticipated that the horizontal current components cancel each other and more uniform current density can be accomplished on the ground plane.

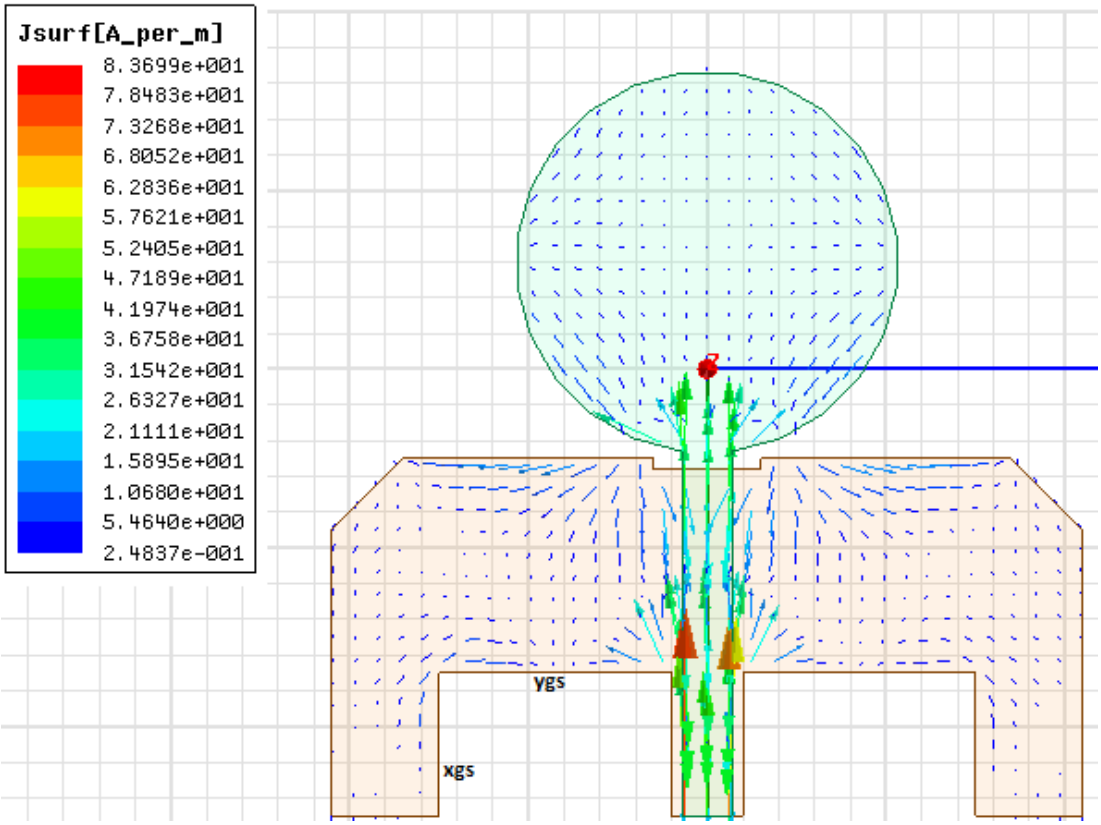

Figure 26: Total current at 9 GHz for ANT 3.

The most suitable notch dimensions (x_{gs}, y_{gs}) for ANT 3, which give the lowest cross polarization without affecting operational bandwidth, are obtained by parametric analyses. The results are given in Figure 27 and Figure 28.

Figure 27 shows co and cross polarization of the ANT 3 for y_{gs} values of 9 mm, 11 mm, and 13 mm ($x_{gs} = 6$ mm). It is found that antenna gives the lowest cross polarization when $y_{gs} = 13$ mm.

Figure 28 shows co and cross polarization for x_{gs} values of 6 mm, 8 mm, and 10 mm ($y_{gs} = 13$ mm). It is seen that when rectangular notch dimensions are x_{gs}=8 mm and y_{gs}=13 mm, the lowest cross polarization is obtained. The cross polarization of the antenna is reduced by 10 dB.

Figure 29 shows s_{11} versus frequency for x_{gs} values of 6 mm, 8 mm, and 10 mm ($y_{gs} = 13$ mm). It is seen that bandwidth of the antenna is not significantly changed when rectangular notch dimensions are x_{gs}=8 mm and y_{gs}=13 mm. However, there is an abrupt change in lower frequency of the ANT 3. There is a notch around 4.3 GHz.

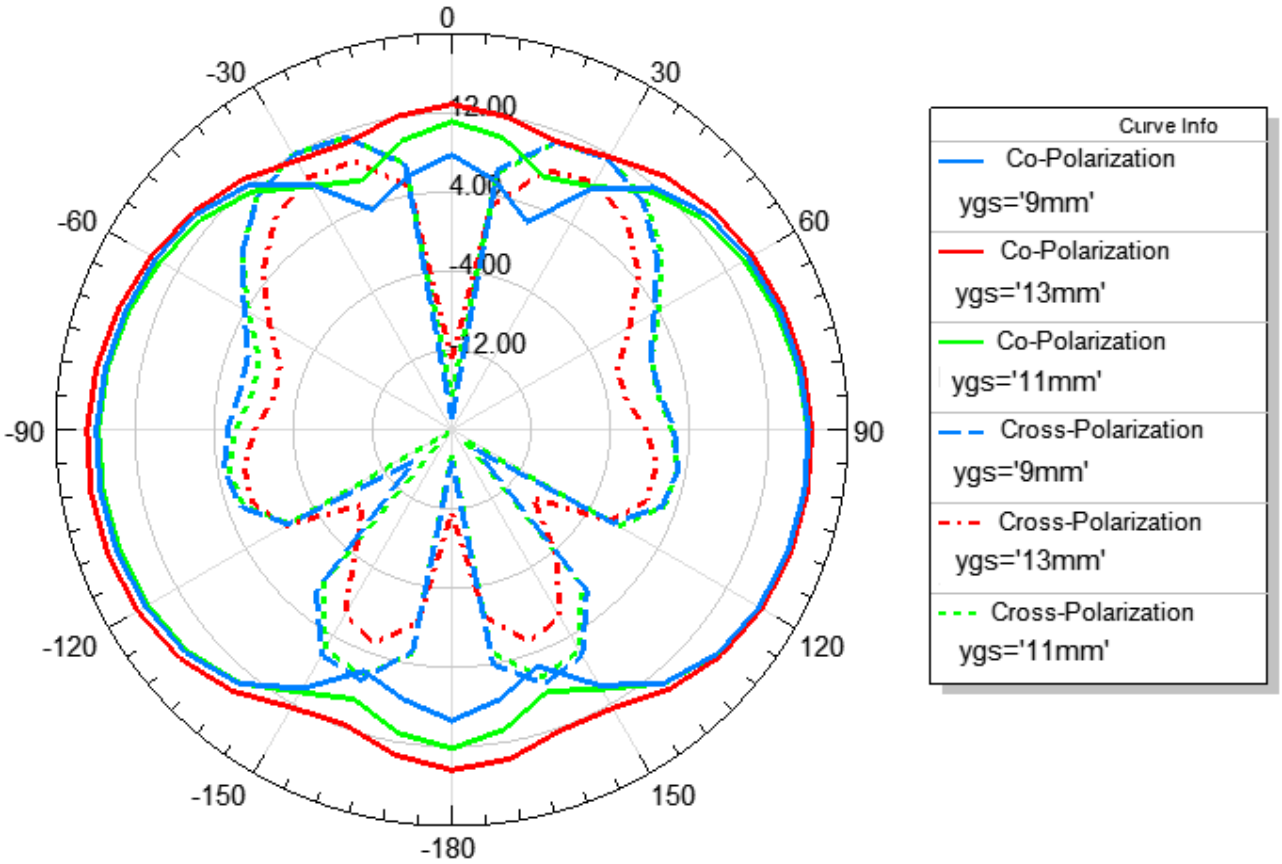

Figure 27: H plane pattern for different y_{gs} (x_{gs}=6 mm).

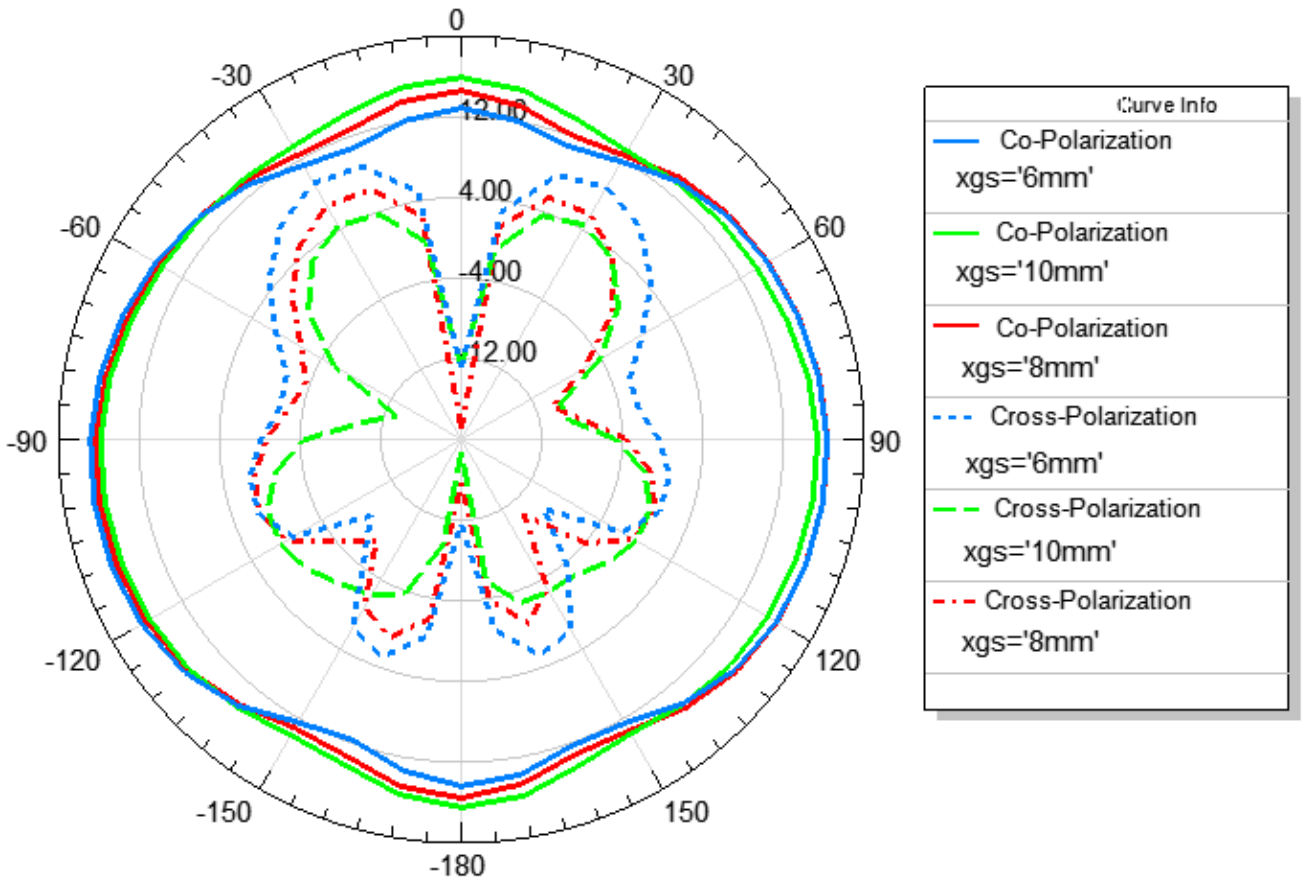

Figure 28: H plane pattern for different x_{gs} (y_{gs}=13mm).

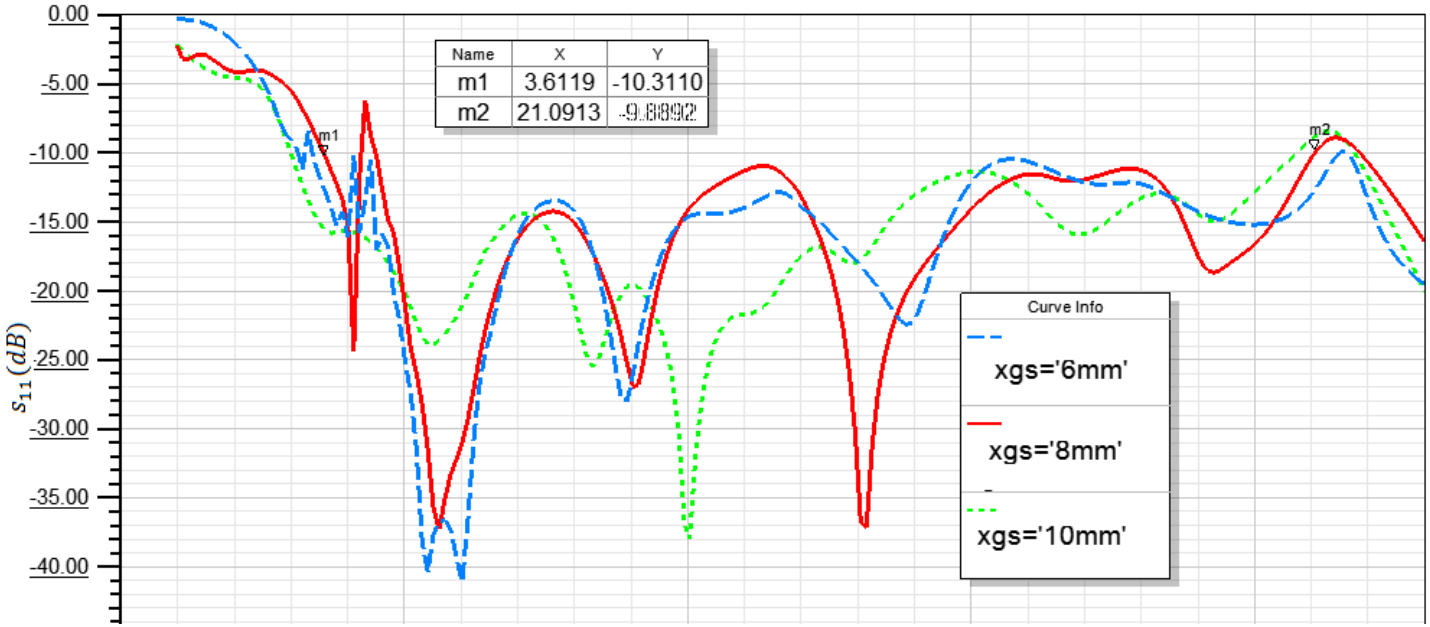

Figure 29: s_{11} versus frequency for different x_{gs} (y_{gs}=13mm).

The resonances in lower frequency of the antenna can be changed by opening circular slot in patch. For this reason, circular slot of radius r_s is opened in the middle of the ANT 3 to obtain ANT 4. With other parameters of the antenna remain fixed, slot size is tuned to 6 mm to obtain a large impedance bandwidth.

The geometry of the ring monopole antenna is depicted in Figure 30.

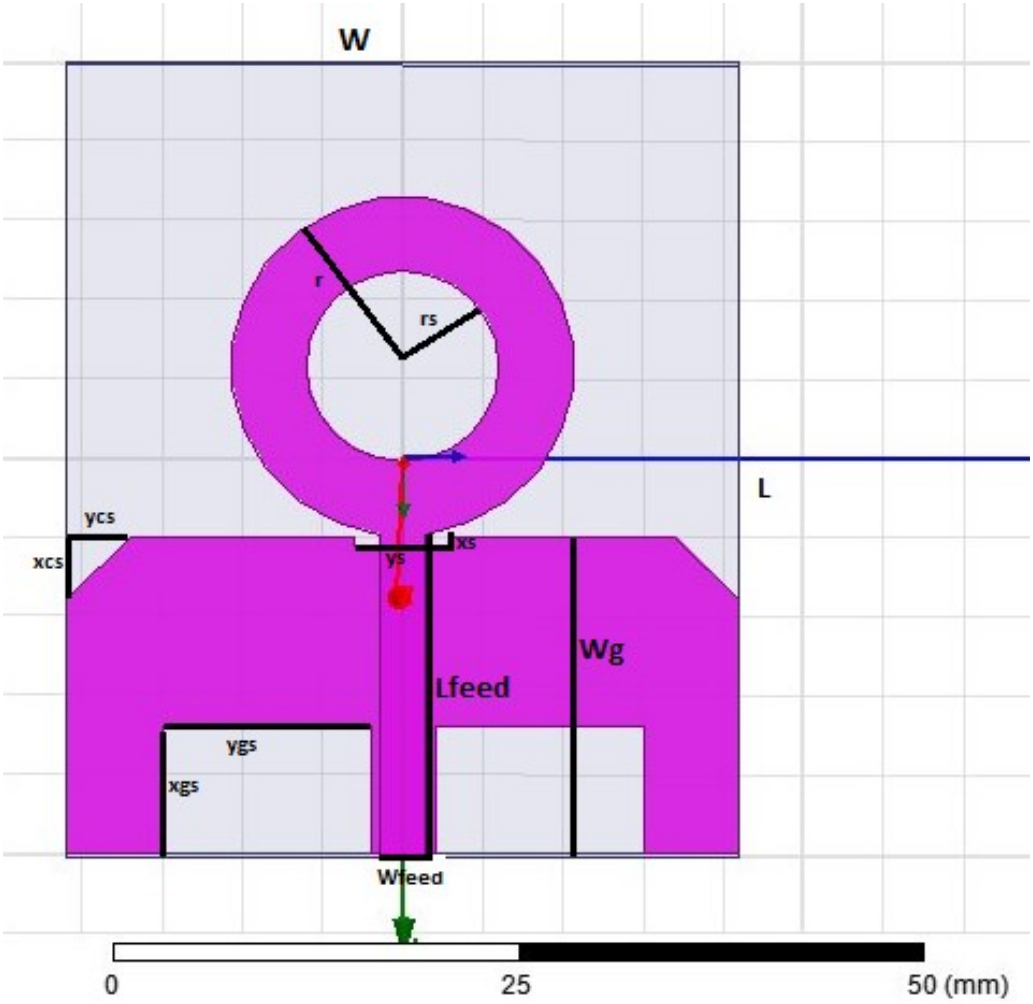

Figure 30: Geometry of UWB ring monopole antenna.

The tuned antenna parameters are given in Table 5.

Table 5: UWB ring monopole antenna parameters

Dimension	Unit (mm)	Dimension	Unit (mm)
L	50	x_{gs}	8
W	42	y_{gs}	13
r	10.7	x_{cs}	4
r_s	6	y_{cs}	4
L_{feed}	20.4	x_s	0.6
W_g	20	y_s	6

The simulated return loss and radiation pattern comparison for ANT 3 and ANT 4 are given in Figure 31 and Figure 32, respectively.

It is seen from Figure 31 that the proposed antenna does not have a notch at 4.3 GHz frequency when the slot is opened. Thus, impedance bandwidth of the antenna is improved in lower band of frequencies.

Figure 32 shows radiation pattern comparison for ANT 3 and ANT 4 on the H plane. It is seen that both antennas have almost the same cross polarization, but ANT 4 has slightly lower cross polarization component compared to ANT 3.

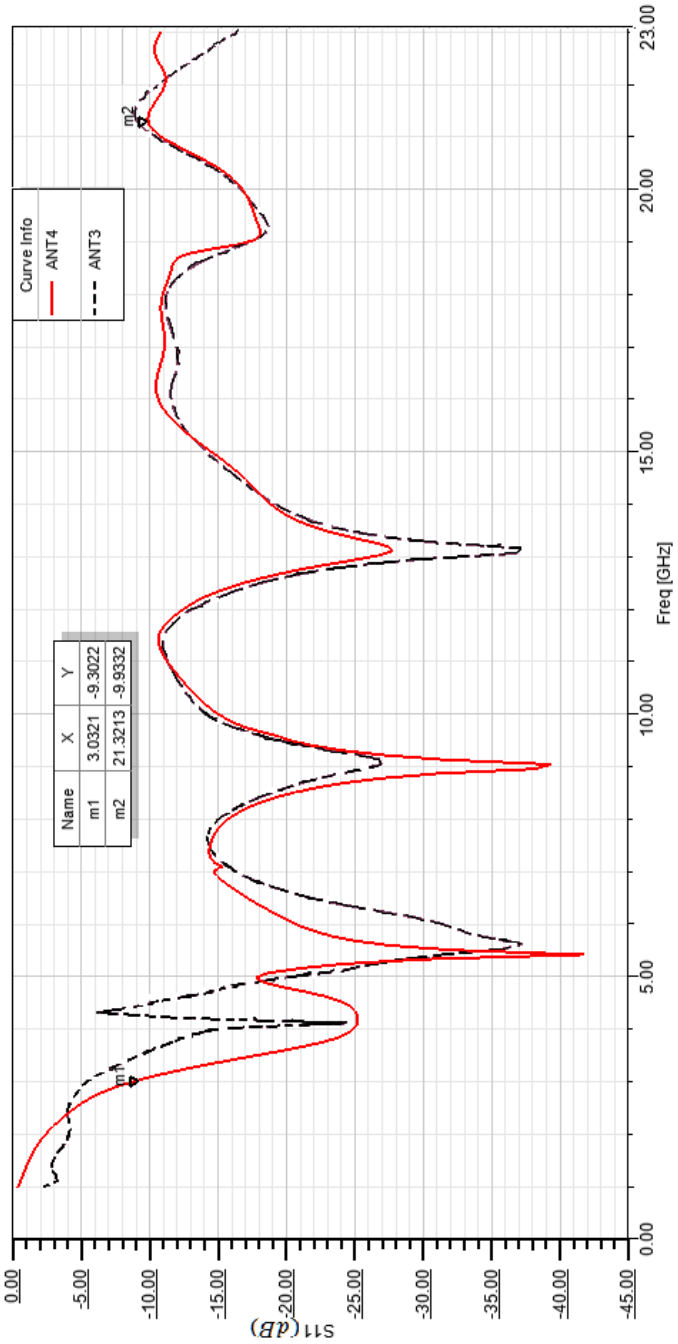

Figure 31: S_{11} versus frequency for ANT 3 and ANT 4.

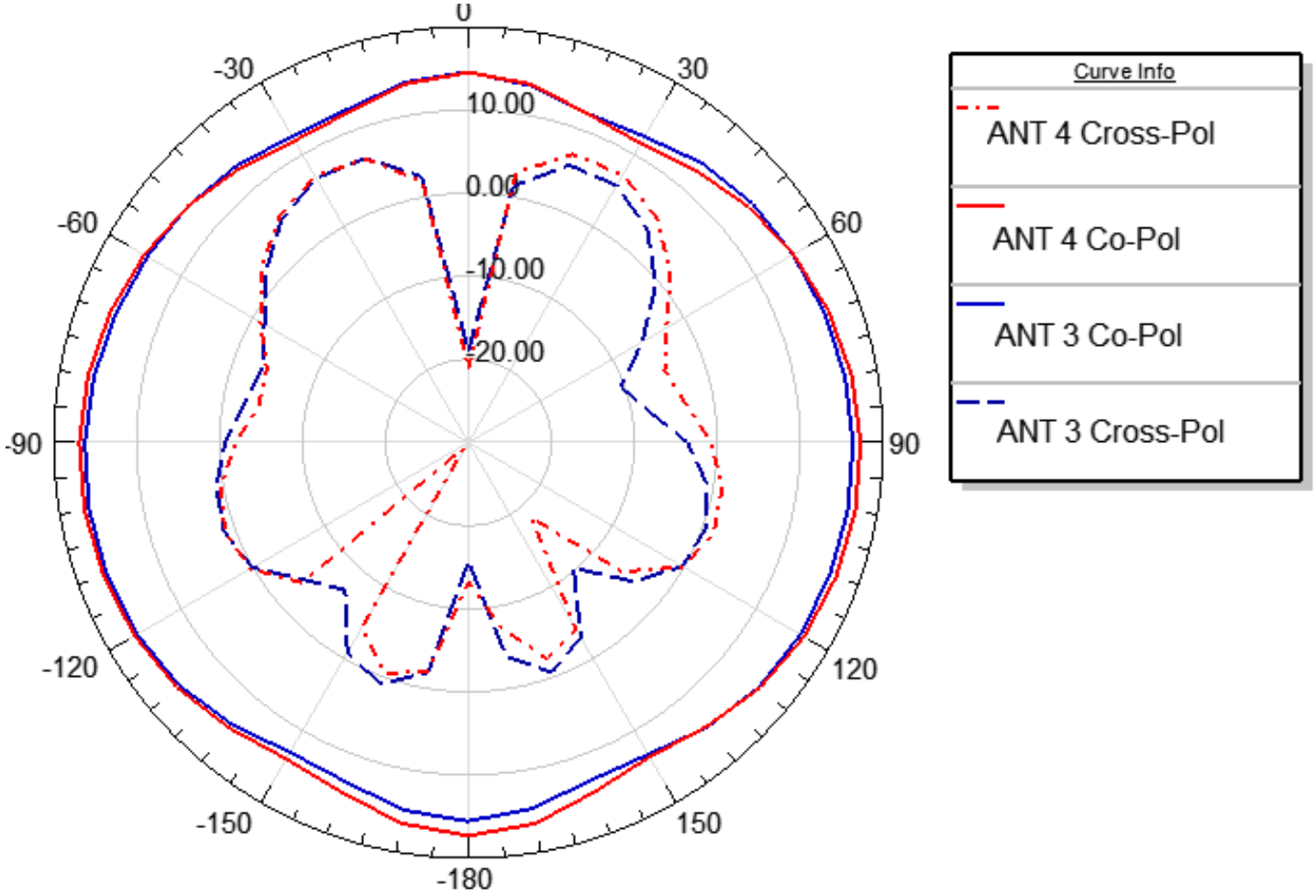

Figure 32: Radiation pattern comparison for ANT 3 and ANT 4 (H plane).

The radiation pattern characteristics of the final design both in E and H plane are given at four different frequencies in Figure 33 and Figure 34. If the variation of the gain of the antenna is less than 3 dB in the operating band, the antenna is considered as an omnidirectional antenna.. It is seen that UWB ring monopole antenna shows omnidirectional pattern on the H plane up to 12 GHz and cross polarization level is less than -20 dB up to 9 GHz. However, cross polarization increases in very high frequencies. The E plane pattern is near-omnidirectional and cross polarization level in E plane is very low at all frequencies.

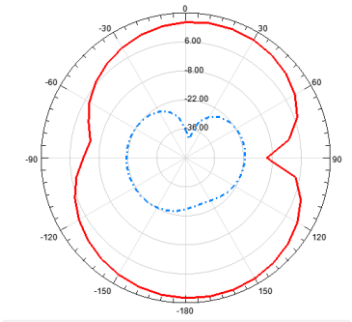

3 GHz (E plane)

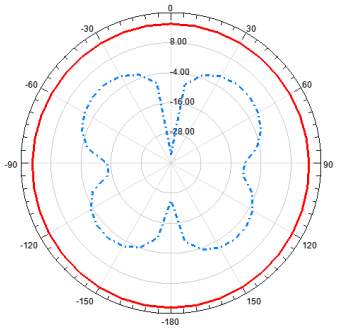

3 GHz (H plane)

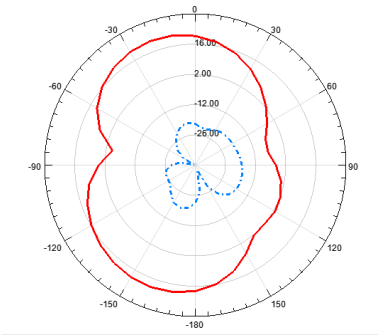

6 GHz (E plane)

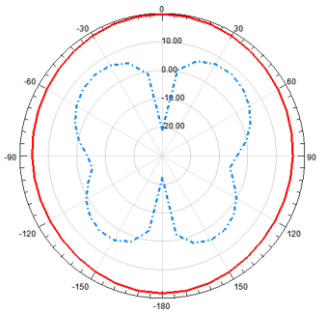

6 GHz (H plane)

Figure 33: Radiation pattern of ring monopole antenna at 3 GHz and 6 GHz.

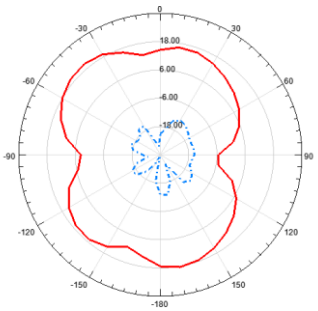

9 GHz (E plane)

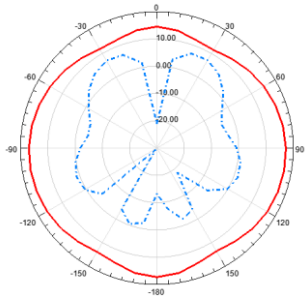

9 GHz (H plane)

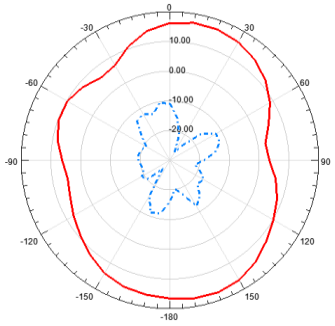

12 GHz (E plane)

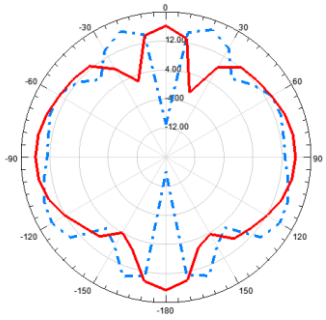

12 GHz (H plane)

Figure 34: Radiation pattern of ring monopole antenna at 9 GHz and 12 GHz

4.2 Design of UWB Monopole Antenna with Symmetrically Parallel Open Circuited Stubs

To improve the radiation characteristics further, structure of the antenna is modified by adding stubs to ground plane as shown in Figure 35.

As mentioned in Section 4.1, the ground plane edge currents around feedline are excessive in simple circular monopole antenna. The aim of this design is to distribute some amount of ground plane current in the symmetrical open circuited stubs, which can improve the radiation patterns of the antenna at high frequencies. The length and width of the open circuited stubs, which gives a large impedance bandwidth, is found with parametric analysis.

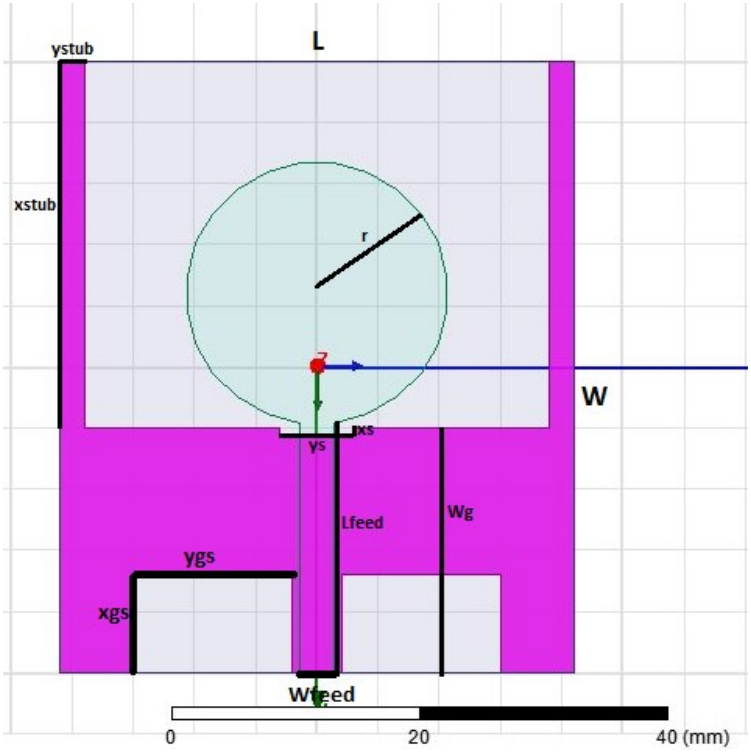

Figure 35: The geometry of the monopole antenna with stubs.

The antenna parameters are given in Table 6.

Table 6: Parameters of UWB monopole antenna with symmetrically parallel open circuited stubs

Dimension	Unit (mm)	Dimension	Unit (mm)
L	50	x_{gs}	8
W	42	y_{gs}	13
r	10.7	x_{stub}	50
L_{feed}	20.4	y_{stub}	2
W_g	20	x_s	0.6
W_{feed}	2.85	y_s	6

The return loss comparison with respect to UWB ring monopole antenna is shown in Figure 36. This antenna has bandwidth of 4.2 GHz-12.3 GHz. Since this antenna does not have tapered edges on top of the ground plane, bandwidth of the antenna is smaller compared to UWB ring monopole antenna.

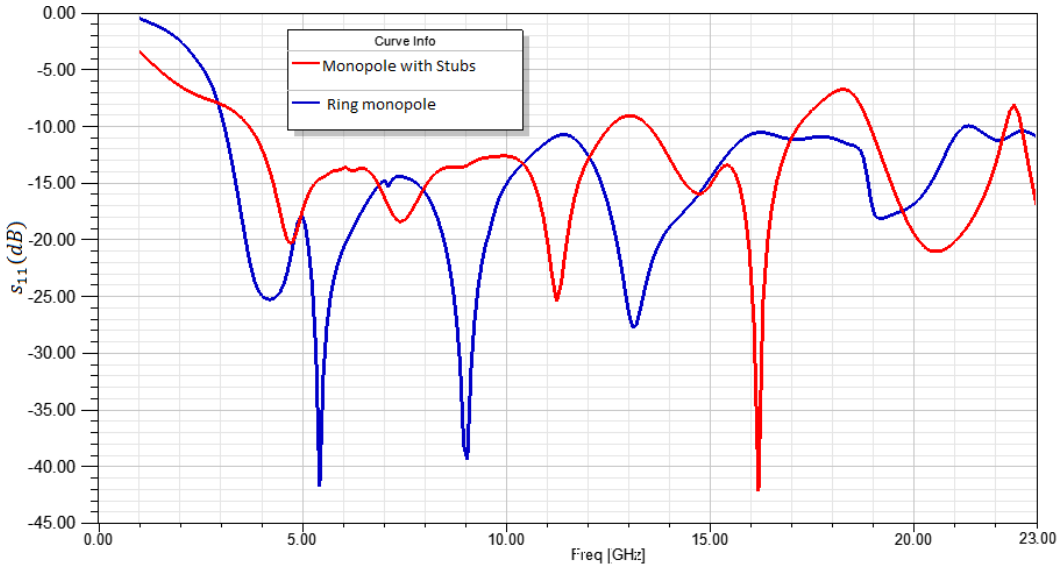

Figure 36: s_{11} versus frequency for ring monopole and monopole with stubs.

The current distribution of antenna, after adding open circuited stubs on ground plane is shown in Figure 37. The horizontal current is very low at low frequencies (4.5 GHz) and more at high frequencies (9 GHz and 11 GHz). After adding open circuited stubs on ground plane, vertical currents are seen on stubs at high frequencies. It is presumed that this modification would result in lower cross polarization at high frequencies, however as seen in Figure 37.c there are still horizontal currents on the top edge of ground plane.

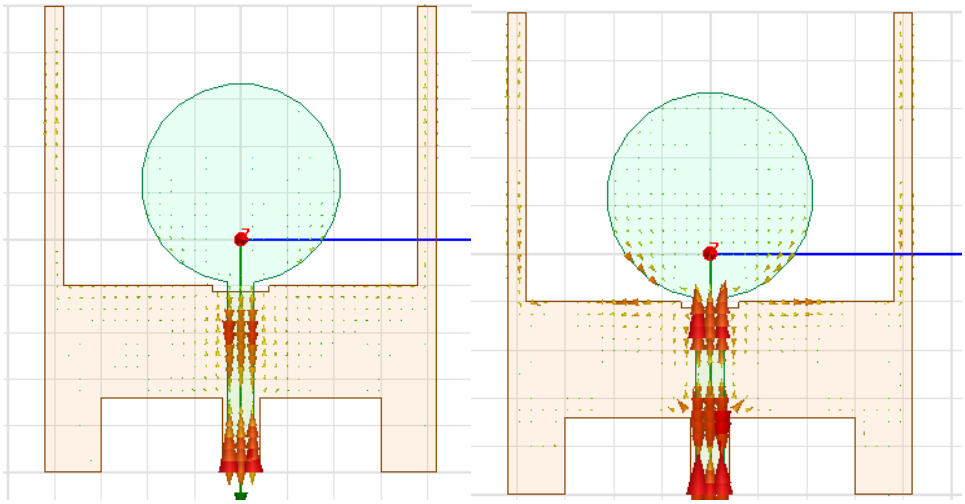

(a) 4.5 GHz (b) 9 GHz

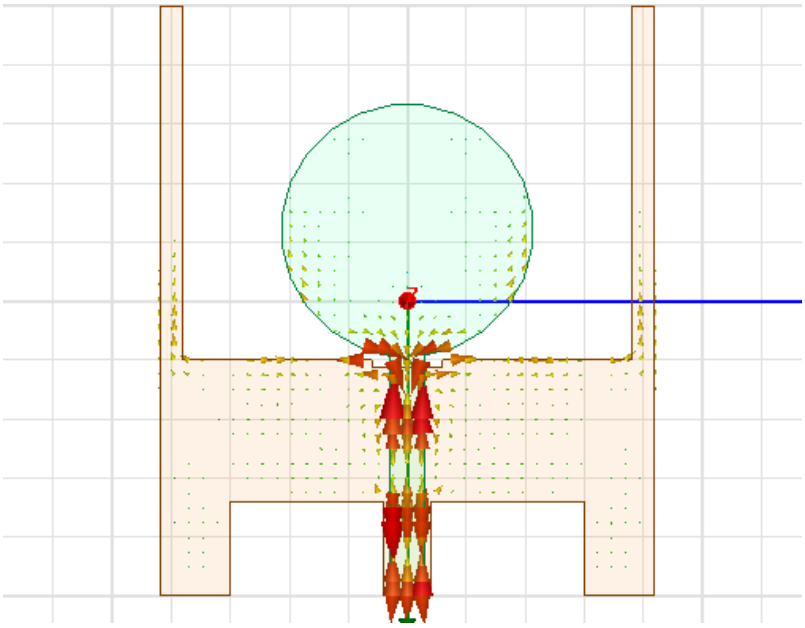

(c) 11 GHz

Figure 37: Current at 3, 9, 11 GHz with open circuited stubs.

The radiation pattern characteristics of antenna are given on four different frequencies in Figure 38. The antenna has omnidirectional pattern on the H plane and omnidirectional characteristics degrade at high frequencies. The cross polarization level is less than -20 dB up to 6 GHz. However, cross polarization

level increases at high frequencies. This design is not as successful as intended. In Section 5.2, comparison of simulated and measured results also proves this observation.

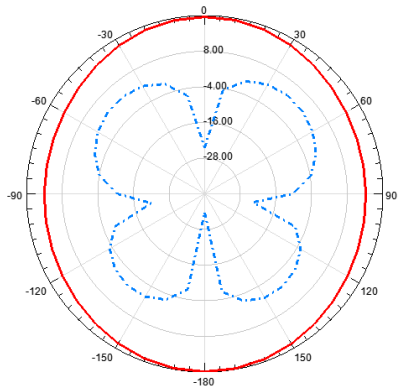

4.3 GHz (H plane)

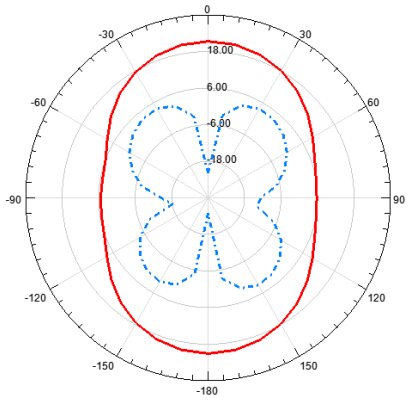

6 GHz (H plane)

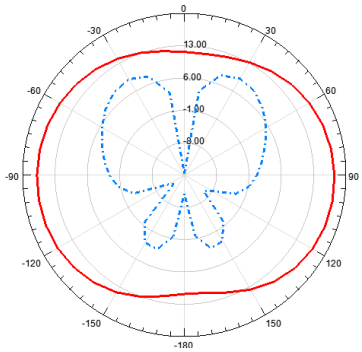

8.5 GHz (H plane)

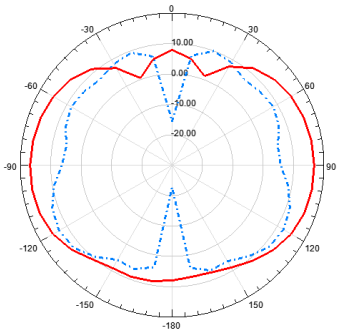

10.5 GHz (H plane)

Figure 38: H plane pattern of antenna

4.3 Design of UWB Antenna with Band Notched Characteristics

In this section, design and simulations of a microstrip line fed circular monopole antenna with ultra-wideband and band-notched characteristics (5 GHz-6.1 GHz) is presented. In literature, several band notched antennas are presented using slits, stubs, slots on the patch and ground plane. In this study, U shaped slot is etched

on feedline to obtain band-notched characteristics. The antenna geometry is given in Figure 39.

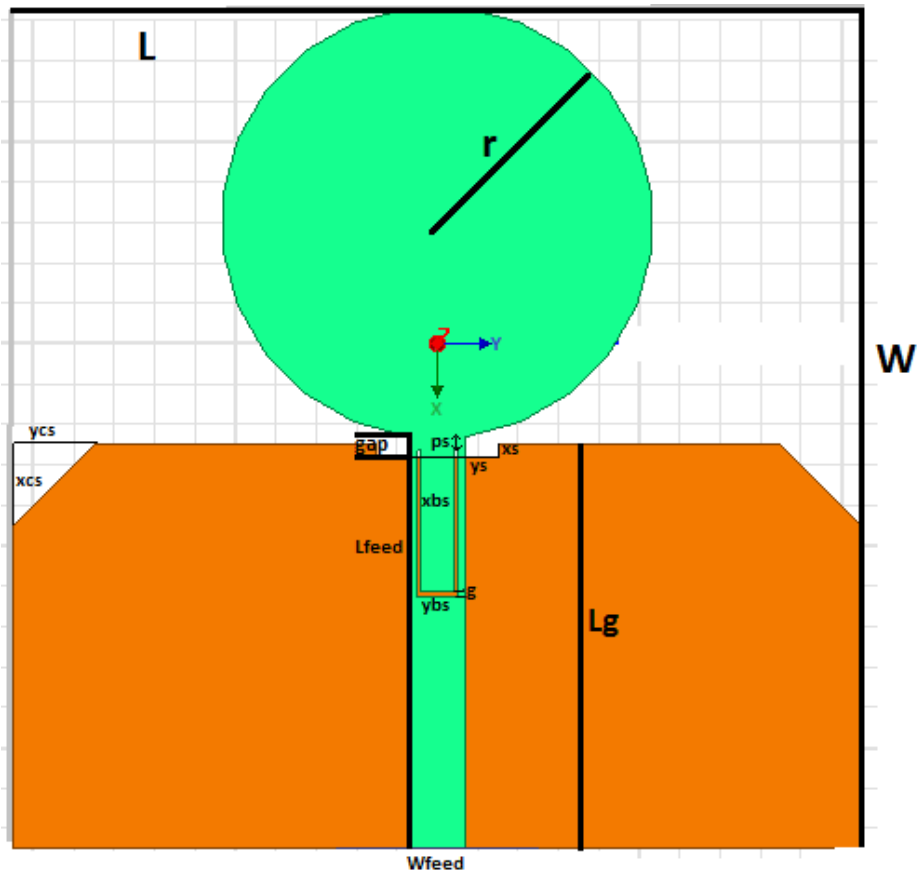

Figure 39: The geometry of UWB band notched antenna.

Antenna parameters are tuned by parametric analyses. The antenna dimensions are shown in Table 7.

Table 7: Parameters of UWB band notched antenna

Dimension	Unit (mm)	Dimension	Unit (mm)
L	50	x_{bs}	7.2
W	42	y_{bs}	1.8
r	10.7	g	0.3
L_{feed}	20.4	x_s	0.6
L_g	20	y_s	6
x_{cs}	4	gap	0.4
y_{cs}	4	p_s	0.2

In order to obtain band-notched antenna characteristics at WLAN (5-6.1 GHz), U slot is etched on the feedline. To obtain band-notched characteristics, a formula given in [16] is used.

$$f_{notch} = \frac{c}{2L\sqrt{\varepsilon_{eff}}}$$

$$\varepsilon_{eff} = \frac{\varepsilon_{r+1}}{2},$$

where 'L' is total length of the U slot, ε_{eff} is the effective dielectric constant and c is speed of light. The first equation is taken into account in obtaining the total length of slot, and then geometry is adjusted for the final design to obtain 5 to 6 GHz notch filter.

The simulated $|S_{11}|$ versus frequency result for ANT 2 and band notched antenna are compared and shown in Figure 40.

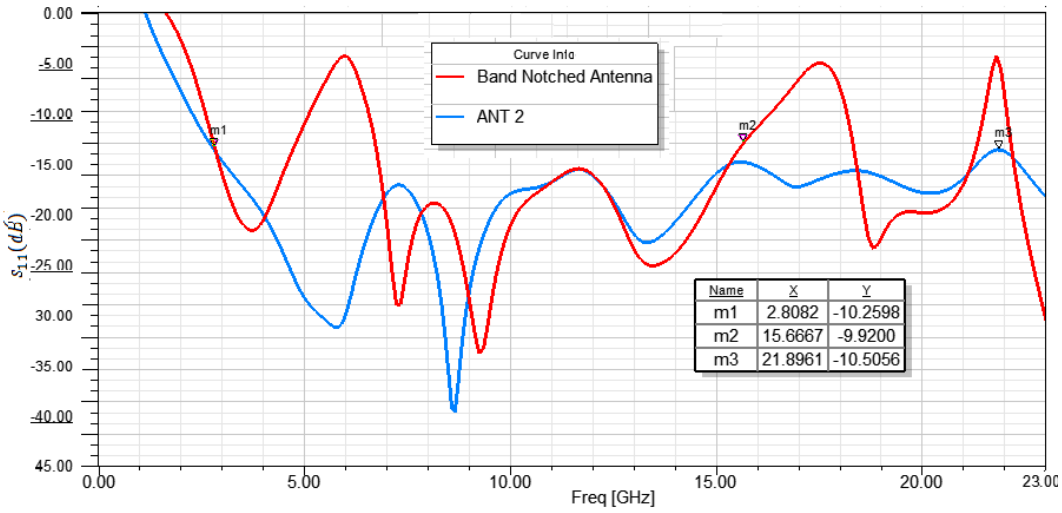

Figure 40: s_{11} versus frequency for ANT 2 and band notched antenna.

Bandwidth of the ANT 2 extends from 2.8 GHz to over 21.8 GHz, while the bandwidth of band notched antenna extends from 2.8 GHz to 15.6 GHz. VSWR of the band notched antenna is less than 2 in entire frequency range except 5– 6.1 GHz band, which represents the WLAN frequencies. At center frequency of the notch band, that is 5.7 GHz, VSWR of the antenna is equal to 5.3.

The performance of band notched antenna depends on some parameters such as the gap between ground plane and patch (*gap*), length (x_{bs}), width (y_{bs}), and the thickness of the U slot (g). From the formula above, the total length of the U slot is found as 16.5 mm, which is also close to 2 x $x_{bs} + y_{bs}$.

Some parametric analyses are carried out to obtain antenna with the largest bandwidth and the highest rejection between 5-6.1 GHz. Figure 41 shows a simulation with different gap (*gap)* distances between ground plane and patch. It is seen that as the gap distance between patch and ground plane changes, impedance bandwidth of the antenna and center frequency of the notch change as well. Appropriate notch frequencies can be adjusted by tuning this parameter. The optimum notch characteristics are obtained when gap distance between patch and ground plane is 0.4 mm.

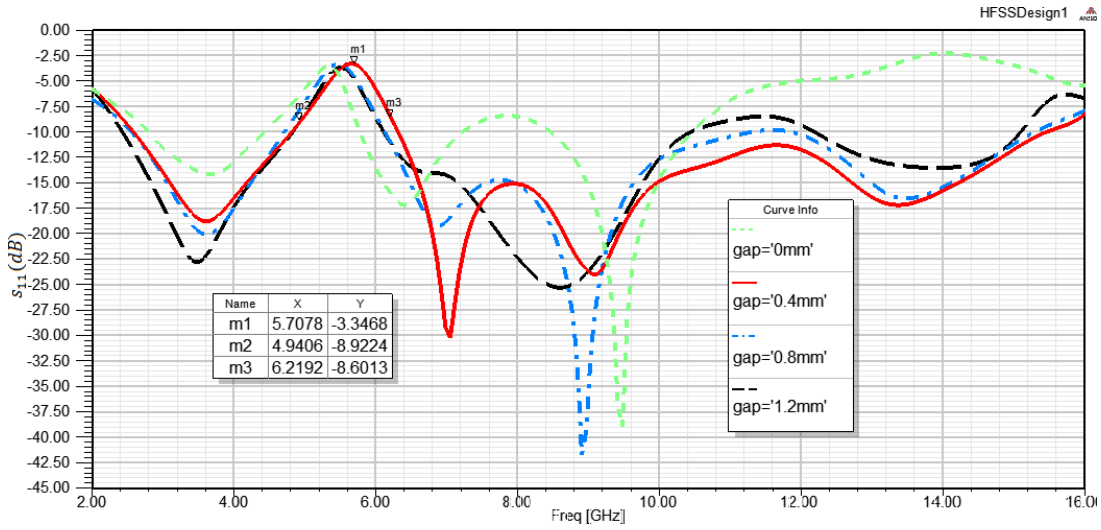

Figure 41: S_{11} versus frequency for different gap distances

The thickness of the U slot also affects impedance bandwidth. Figure 42 shows a simulation with different U slot thickness values. It is seen that as U slot thickness increases, notch frequency shifts to higher frequencies. It is further seen that for small value of thickness of 0.1 mm, there is no notch frequency. The good bandwidth and band notched characteristics are obtained for gap value of 0.3 mm.

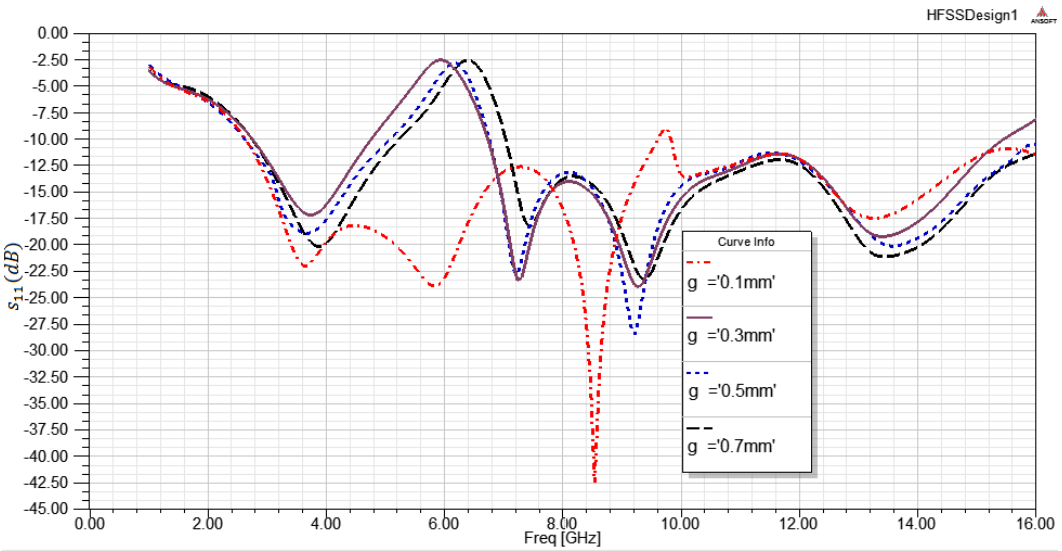

Figure 42: s_{11} versus frequency for different U slot thickness values.

The U slot is initially designed at a random place on the feedline. The best position of the U slot is found by moving the slot over the feedline and by parametric analyses. Distance from the junction of circular patch and feedline to the top of U slot is defined as p_s. The effect of position of U slot to bandwidth characteristics is plotted in Figure 43. When U slot gets close to the patch, the notch frequencies become narrower and notch center frequency shifts to lower frequencies. The notch bandwidth increases as U slot moves away from the patch.

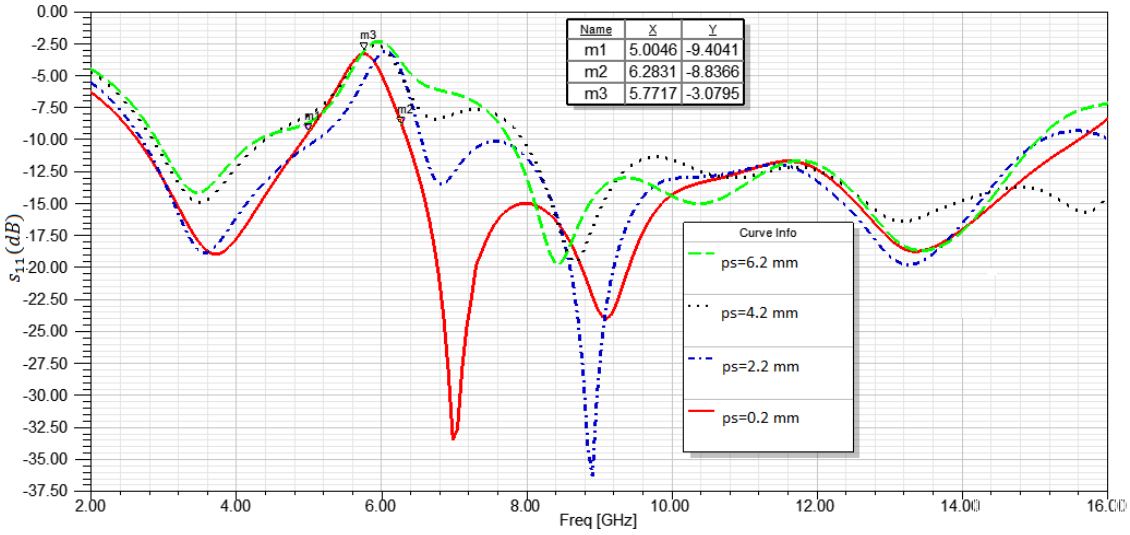

Figure 43: s_{11} versus frequency for different positions of U slot.

Figure 44 shows the simulated current distribution on the notched antenna at 3 GHz, 5.7 GHz and 8 GHz, respectively. It can be observed that less current is flowing into circular patch at the notch frequency. Therefore, the antenna does not radiate effectively at this frequency.

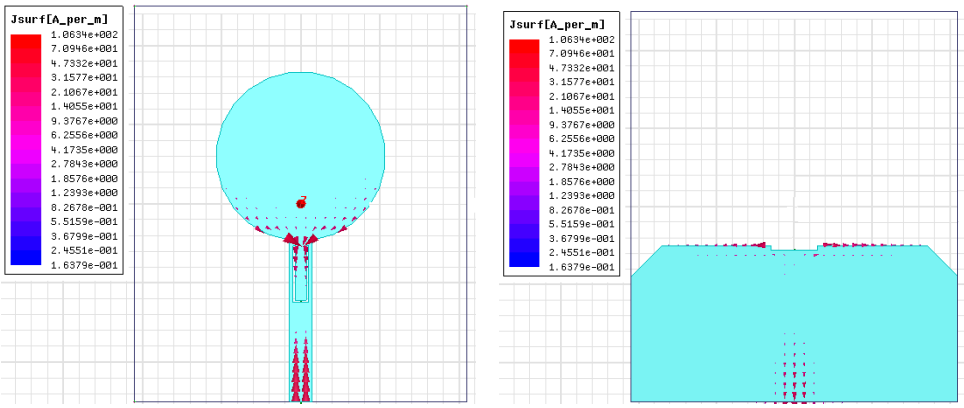

(a) 3 GHz

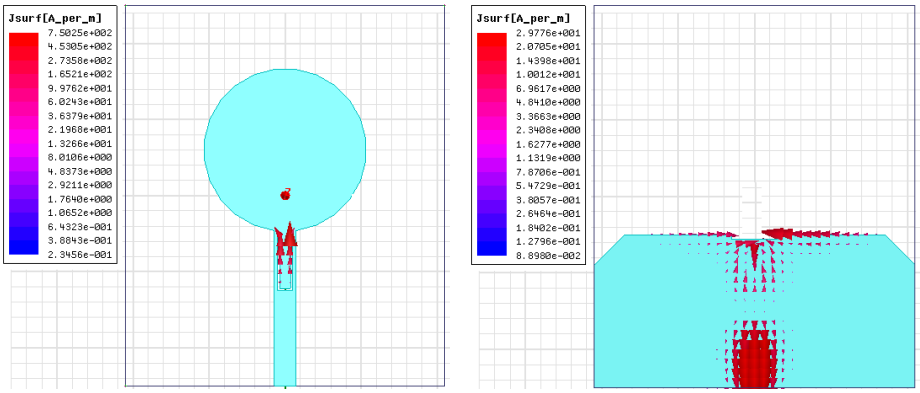

(b) 5.7 GHz

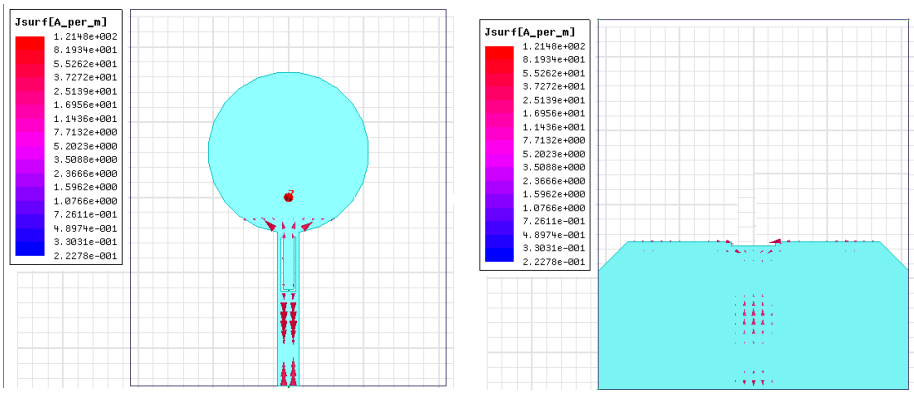

(c) 8 GHz

Figure 44: Simulated surface current distribution of band notched antenna.

Gain versus frequency graph for the band notched antenna and ANT 2 is compared and shown in Figure 45. It is observed that gain decreases significantly, at notch frequencies.

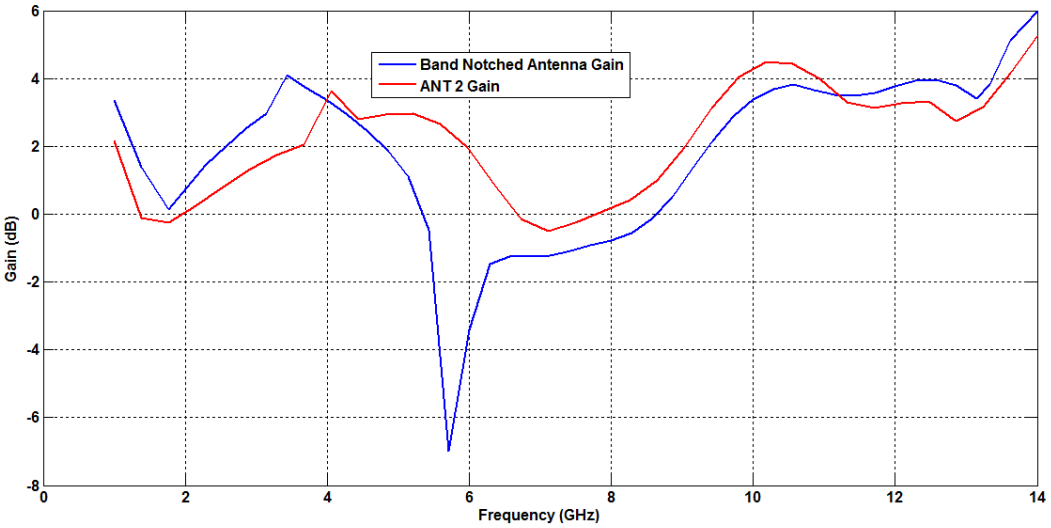

Figure 45: Gain versus frequency for band notched antenna and ANT 2.

Radiation pattern characteristics of the final design are given at three different frequencies in Figure 46. The antenna shows omnidirectional pattern on the H plane up to 7 GHz. The cross polarization level is low up to 7 GHz, and cross polarization level becomes very high at high frequencies. The antenna has near-omnidirectional pattern on the E plane and the cross polarization level is low at all frequencies.

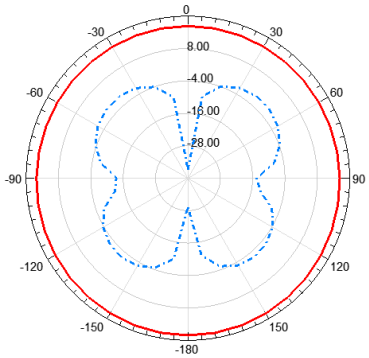

3 GHz (H plane)

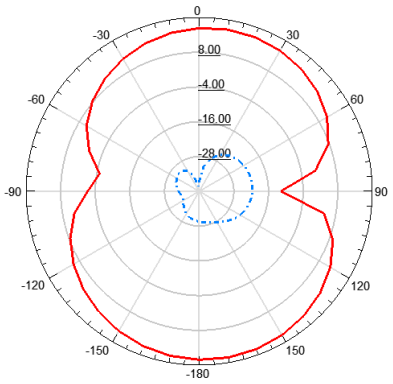

3 GHz (E plane)

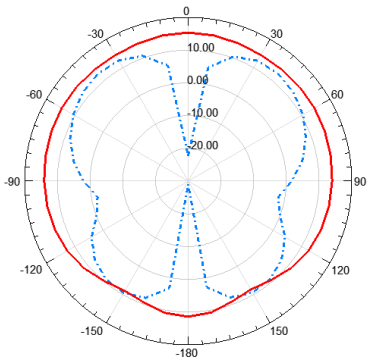

7 GHz (H plane)

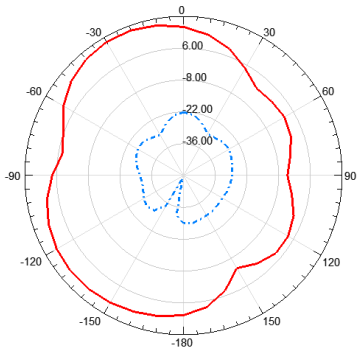

7 GHz (E plane)

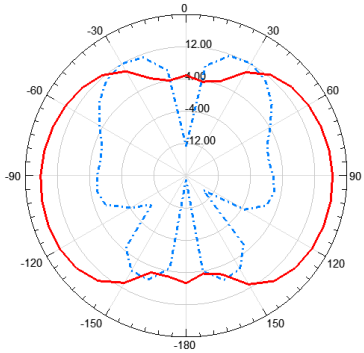

9 GHz (H plane)

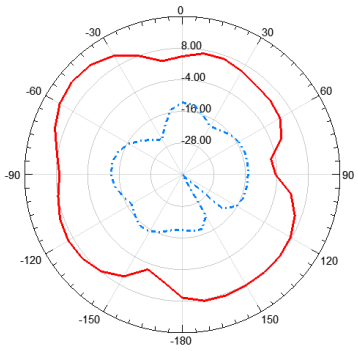

9 GHz (E plane)

Figure 46: Radiation pattern of UWB band notched antenna

CHAPTER 5

COMPARISON OF SIMULATED AND MEASURED RESULTS

Antennas designed in Chapter 4 are produced, characteristics measured and presented in this chapter by comparison with the simulation results. Moreover, the proposed antennas are compared with similar antennas available in literature. The antennas are fabricated using PCB LPKF prototyping machine.

5.1 Comparison of Measurement and Simulation Results for Ultra-Wideband Ring Monopole Antenna

The UWB ring monopole antenna is designed and analyzed in Section 4.1. Three antennas are produced and tested because manufacturing errors may affect the antenna bandwidth. The photos of the manufactured antennas are shown in Figure 47. In the second antenna, there is a scratch on the top of the substrate. Two antennas are tested with the same connector and the other is tested with different connector.

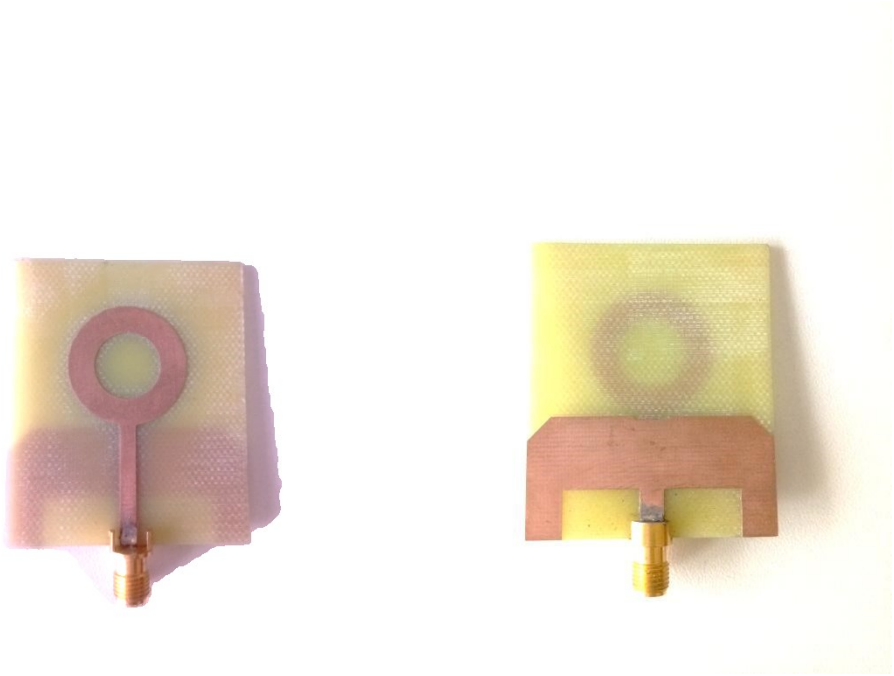

(a) top view (b) bottom view

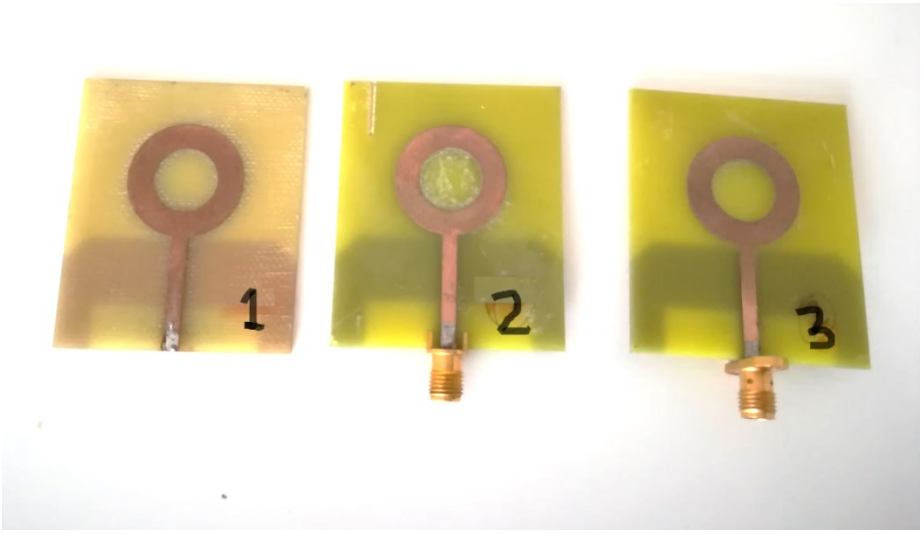

(c) fabricated antennas

Figure 47: Photographs of UWB ring monopole antennas.

The measured and simulated return loss characteristics of the proposed antennas are compared in Figure 48.

It is observed that all antennas have UWB characteristics. However, Antennas 1 and 2 have higher s_{11} values, slightly greater than -10 dB between 11-15 GHz compared to Antenna 3.

It is seen that there are some differences between the measured and simulated return loss results in some frequencies. The differences between simulated and measured results are due to the fabrication errors, effect of SMA connectors and fluctuation of FR4 permittivity over a wide range of frequencies.

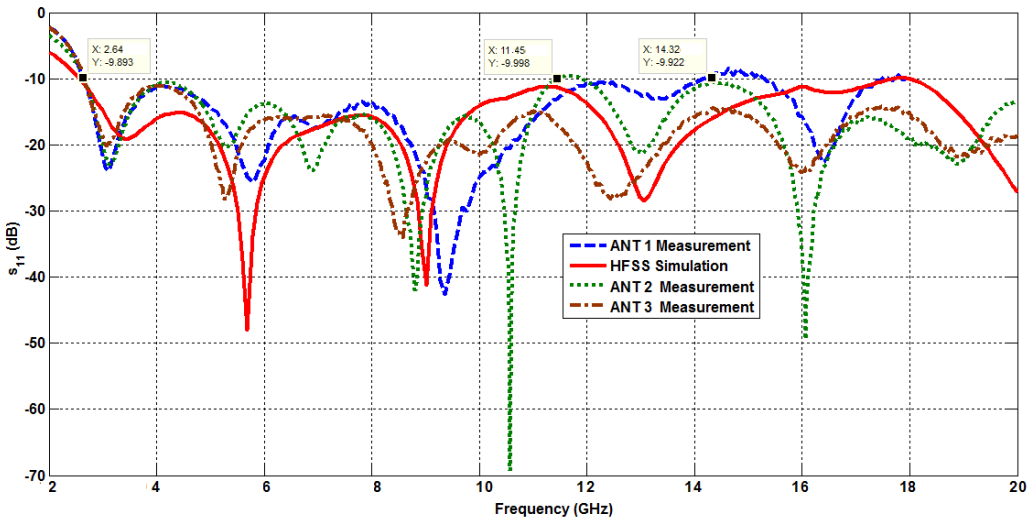

Figure 48: s_{11} versus frequency for measured and simulated results.

The simulations are performed by using wave port or lumped port excitation. However, in measurement, SMA connectors are used. The connectors introduce mismatch and a phase shift. For fair comparison between measured and simulated results, simulations are also performed by using SMA connector, and the results are presented in Figure 49. As seen, simulation with SMA connector has a significant effect on the bandwidth of the antenna. It is observed that simulation results for antenna with connector are closer to the measured ones.

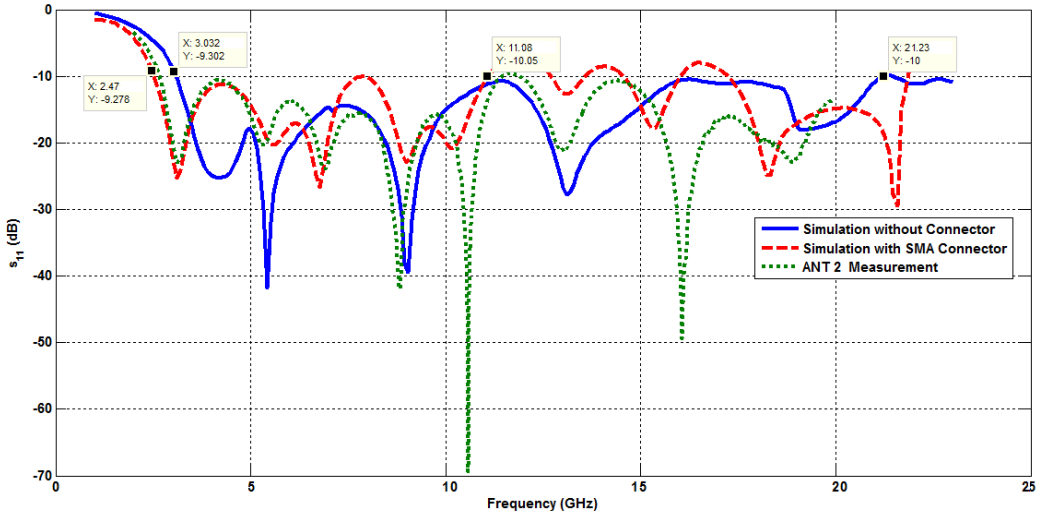

Figure 49: s_{11} versus frequency results with SMA connector.

Radiation pattern of the antennas are measured in the anechoic chamber with far-field set up in the METU Department of Electrical and Electronics Engineering. The measured and simulated radiation pattern characteristics for UWB ring monopole antenna 3 in H and E planes are compared in Figure 50 and Figure 51, respectively.

As can be seen in Figure 50, in the operating frequency band, the proposed antenna exhibits omnidirectional radiation pattern in the H-plane. The measured cross-polarization level of the designed antenna is lower than -10 dB up to 9 GHz. Simulated and measured patterns agree each other at low frequencies. There are small differences for higher frequencies.

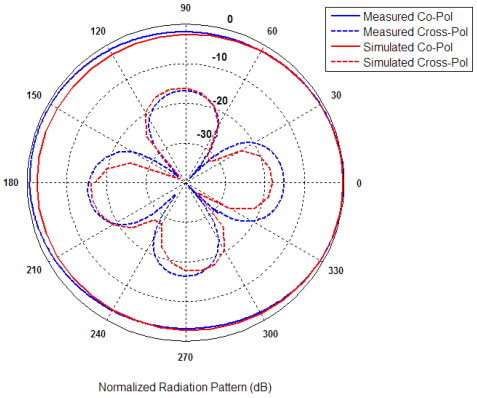

(a) 3 GHz

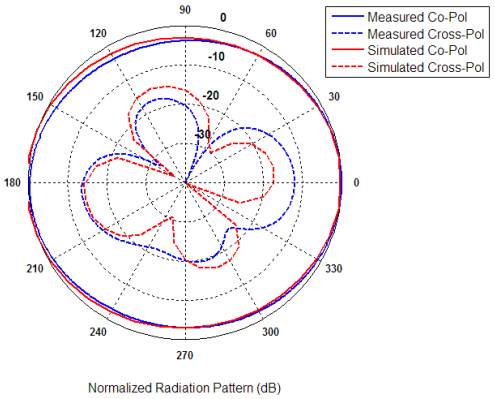

(b) 5.5 GHz

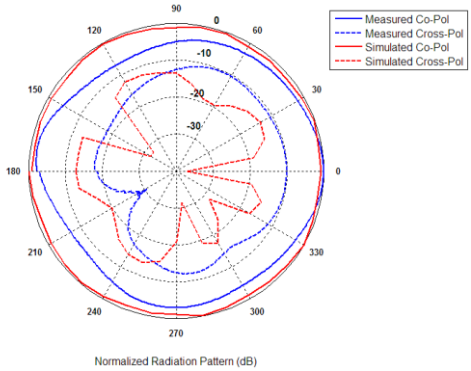

(c) 9 GHz

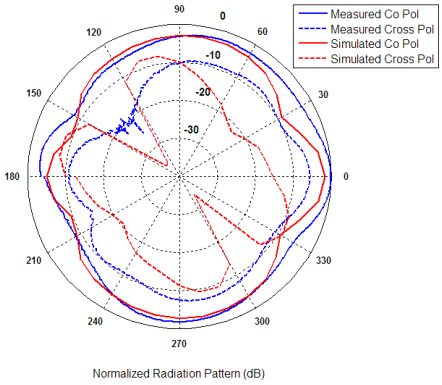

(d) 11 GHz

Figure 50: Measured and simulated H(y-z) plane pattern comparison.

Figure 51 shows measured and simulated E(x-z) plane radiation patterns comparison for UWB ring monopole antenna at 3, 5.5, 9, 11 GHz. It is observed that the proposed antenna exhibits near-omnidirectional radiation pattern in the E-plane. The measured cross polarization is low at all frequencies and it increases at high frequencies.

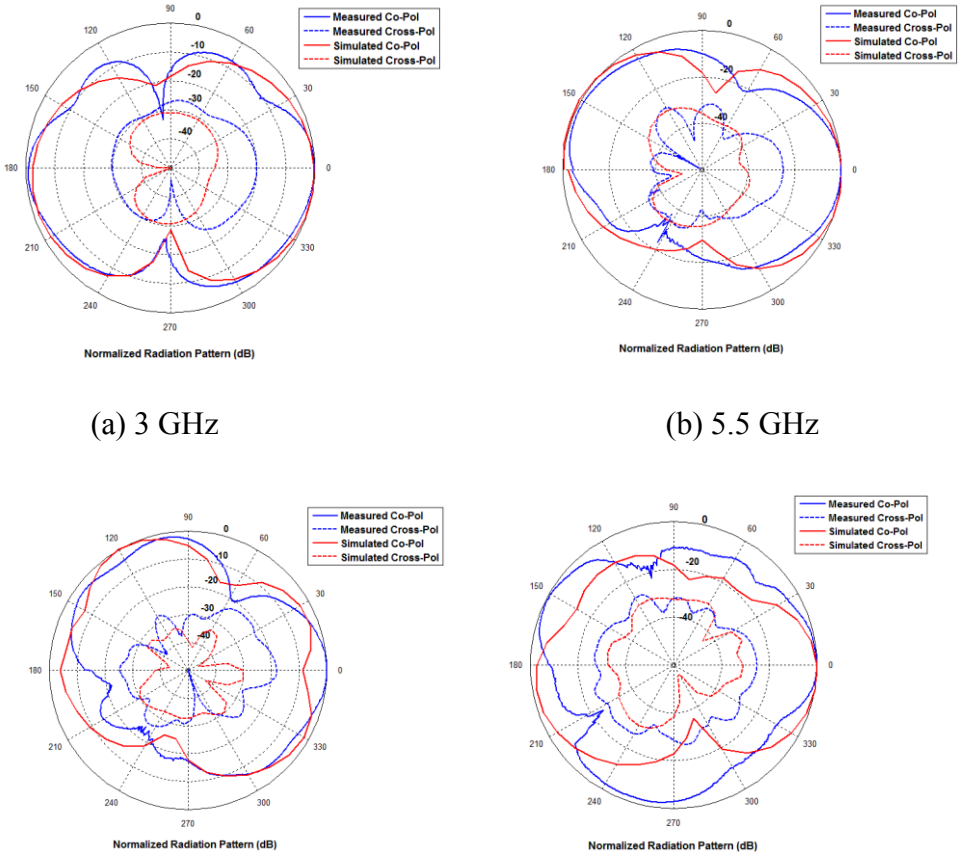

(a) 3 GHz (b) 5.5 GHz

(c) 9 GHz (d) 11 GHz

Figure 51: Measured and simulated E(x-z) plane pattern comparison.

The bandwidth and size of the similar antennas in the literature are compared with those of the proposed antenna in Table 8. Although the size of the proposed antenna is almost same as the sizes of antennas in literature, it is bandwidth is wider.

Table 8: Comparison of reference designs with UWB ring monopole antenna

Reference	**Dimension (mm^2)**	**Substrate Height (h)**	**Dielectric Constant (ε)**	**Bandwidth ($\lvert s_{11}\rvert$< -10 dB)**	**Peak Gain (dB)**
[10]	40x30	1.59	4.4	3.1–10 GHz	NA
[11]	50x42	1.5	4.4	2.69–10.16 GHz	6.2
[12]	42x42	1.5	4.7	2.6–10.6 GHz	7
Proposed Antenna	50x42	1.6	4.4	2.6–20 GHz	6.9

5.2 Comparison of Measurement and Simulation Results for UWB Monopole Antenna with Symmetrically Parallel Open Circuited Stubs

The UWB monopole antenna with symmetrically parallel open circuited stubs is designed and analyzed in Section 4.2. The antenna is produced and tested. The photos of the manufactured antenna are shown in Figure 52.

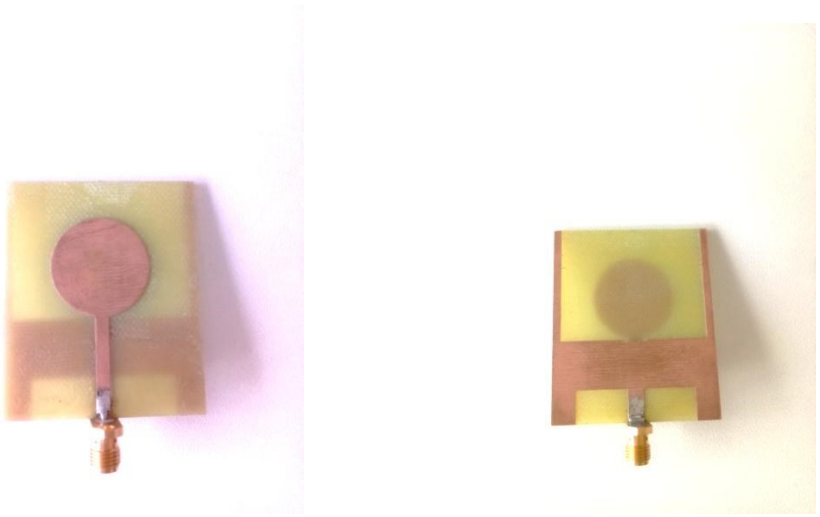

(a) top view (b) bottom view

Figure 52: Photographs of produced antenna.

The measured and simulated return loss characteristics of the proposed antenna are compared and shown in Figure 53. The fabricated antenna has a frequency band from 4.3 GHz to 11.2 GHz, whereas bandwidth of the simulated one is between 4.3 and 12.5 GHz. The differences between the measured and simulated results may be due to fabrication errors, effect of SMA connector and the fluctuation of FR4 permittivity over wide range of frequencies.

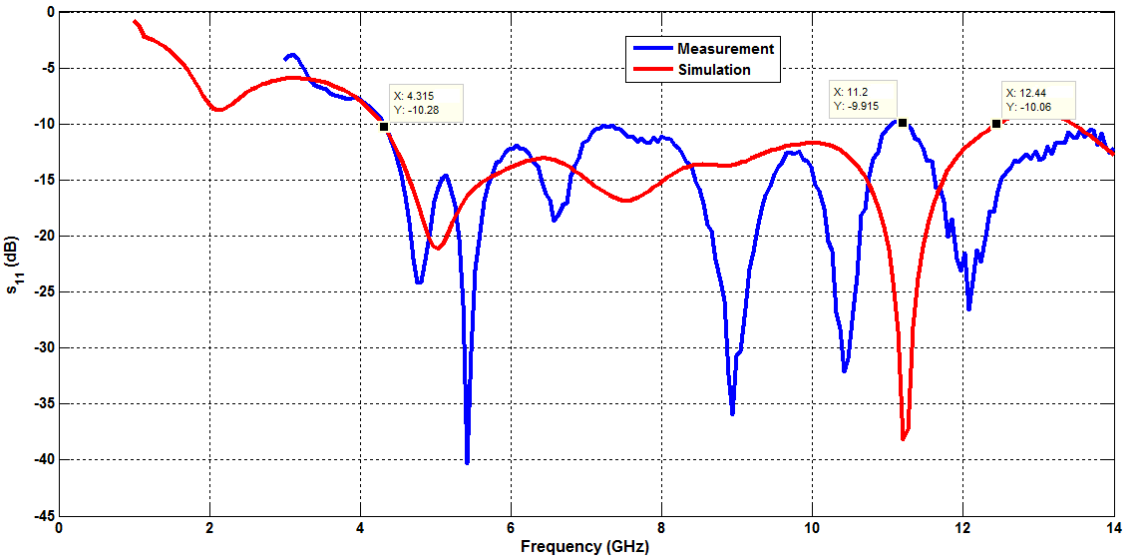

Figure 53: s_{11} versus frequency for measured and simulated results.

The measured and simulated radiation pattern characteristics of the antenna are shown in Figure 54. It can be seen that the antenna exhibits poor omnidirectional characteristics in the H-plane. The measured cross-polarization level of the designed antenna is lower than -10 dB up to 8 GHz. For frequencies higher than 8 GHz, cross polarization level is high. This design has poor performance compared to UWB ring monopole antenna and the previous studies. It can be concluded that, the parallel strip lines on the ground plane may have a negative effect on the radiation of patch antenna.

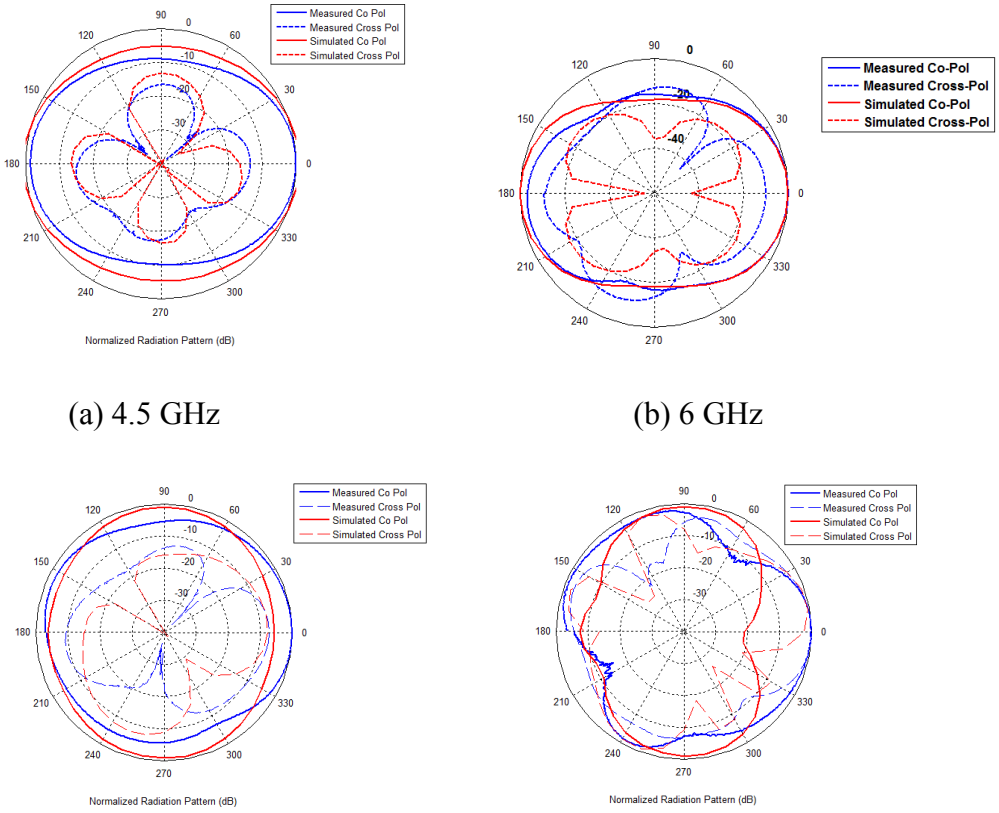

(a) 4.5 GHz (b) 6 GHz

(c) 8 GHz (d) 11 GHz

Figure 54: Measured and simulated pattern comparison (H plane).

5.3 Comparison of Measurement and Simulation Results for UWB Antenna with Band Notched Characteristics

Two samples of UWB band notched antennas are produced and tested to observe the effect of manufacturing errors on the antenna bandwidth. The photos of the manufactured antennas are shown in Figure 55.

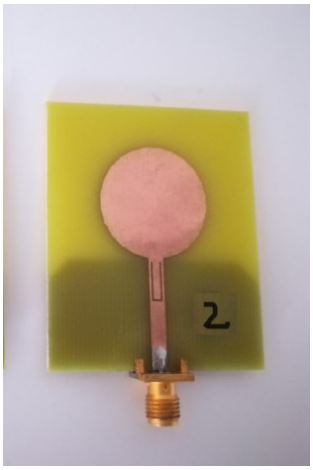

(a) top view

(b) bottom view

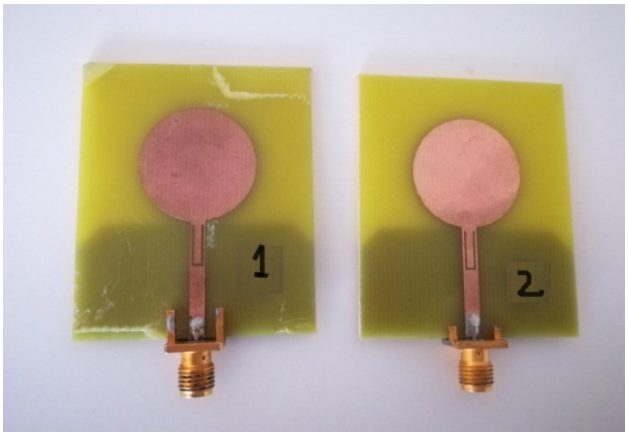

(c) fabricated antennas

Figure 55: Photograph of the band notched antenna.

The measured and simulated return loss characteristics of the proposed antennas are compared and shown in Figure 56. The first fabricated antenna has the frequency band from 2.5 GHz to 10.6 GHz with WLAN stopband frequency of 4.9-7.1 GHz. The second fabricated antenna has the frequency band from 2.5 GHz to 16.5 GHz with WLAN stopband frequency of 4.9-6.5 GHz. The comparison among monopole antennas shows that the second antenna has the better performance.

It is seen that there are some differences between the measured and simulated return loss results after some frequencies. The differences between simulated and measured results are due to the fabrication errors, effect of SMA connectors and fluctuation of FR4 permittivity over a wide range of frequencies.

The dimensions of the U slot are measured in order to see if there is any manufacturing error. The band notched antenna is designed with 300 µm U slot thickness. By using micrometer, U slot thickness of the first antenna is measured as 420 µm, whereas U slot thickness of the second antenna is measured as 320 µm. U slot thickness of the second antenna is very close to intended value, which also explains why the second antenna shows better performance compared to first one.

Simulations are also performed by using SMA connector in order to observe the effect of the SMA connectors in measurements. As seen in Figure 56, simulation with SMA connector has significant effect on the bandwidth of the antenna. It is observed that simulation results with connector are closer to the measured ones.

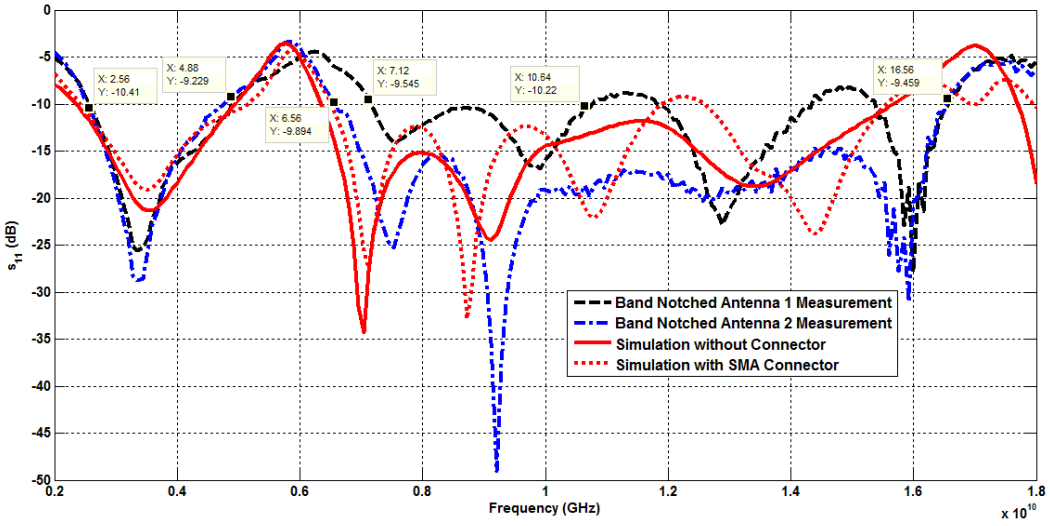

Figure 56: s_{11} versus frequency for measured and simulated results.

The measured and simulated radiation pattern characteristics for band notched antenna 2 are compared in Figure 57.

As can be seen in Figure 57, the proposed antenna exhibits omnidirectional radiation pattern in the H-plane at 3.5 GHz, however omnidirectional characteristic is distorted at higher frequencies 7.5 and 10 GHz. The measured H-plane cross-polarization level of the proposed antenna is lower than -10 dB at 3.5 GHz. However, cross polarization level increases at high frequencies.

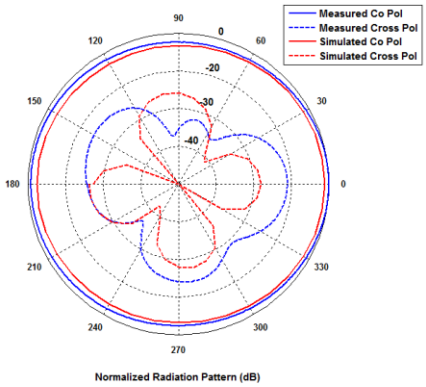

(a) 3.5 GHz

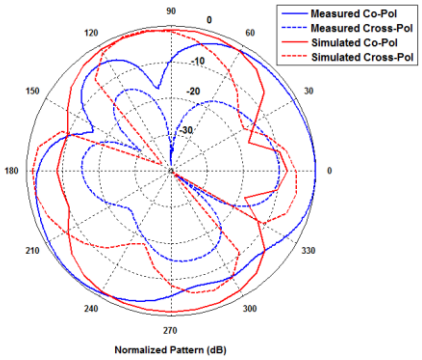

(b) 7.5 GHz

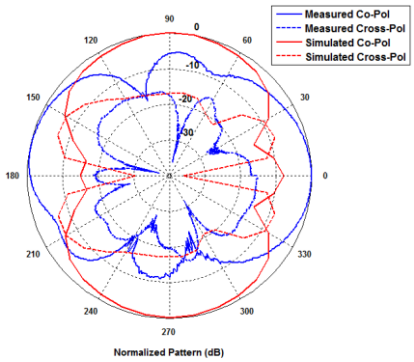

(c) 10 GHz

Figure 57: H plane pattern comparison for UWB band notched antenna.

The bandwidth and size of the similar antennas in literature are compared with those of the proposed antenna in Table 9. As seen, the proposed antenna has larger size, wide bandwidth and large peak gain when compared to the previous studies.

Table 9: Comparison of reference designs with UWB band notched antenna

Reference	**Dimension (mm^2)**	**Substrate Height (h)**	**Dielectric Constant (ε)**	**Bandwidth ($\lvert s_{11}\rvert$< -10 dB)**	**Peak Gain (dB)**	**Notch Frequency**
[13]	30x33	1.6	4.4	3.1–10.6 GHz	NA	3.1–4.7 GHz
[14]	25x30	1.5	4.4	3–12 GHz	4.5	5.4–6.4 GHz
Proposed Antenna	50x42	1.6	4.4	2.5–16.5 GHz	5.5	4.9–6.5 GHz

CHAPTER 6

DISCUSSION AND CONCLUSION

There are many studies in the literature which investigate UWB antennas and band notched antennas. Several antenna designs were investigated before starting this thesis. Considerable part of these designs achieve UWB antenna. However, some of them have poor omnidirectional radiation pattern and high cross polarization at high frequencies. Moreover, the band notched antennas in previous works do not have large bandwidth.

In this study, three UWB antennas are proposed. UWB ring monopole antenna, UWB antenna with parallel strip lines and UWB band notched antenna are designed and analyzed. First, a simple circular monopole antenna is designed. Effect of the antenna parameters to bandwidth enhancement is investigated by using parametric analyses. After this study, design guidelines are proposed for simple circular monopole antenna. The designed simple circular monopole antenna has a relatively smaller bandwidth and poor radiation characteristics. We aimed to have large bandwidth with omnidirectional radiation pattern and low cross polarization. For this purpose, various methods are applied for both bandwidth enhancement and radiation pattern improvement. The antennas are manufactured and radiation characteristics are measured. The measured return loss, co polarized and cross polarized radiation patterns results are compared with simulation results.

First, a microstrip line fed UWB ring monopole antenna is presented. The impedance bandwidth of the antenna is successfully improved in the lower frequency band by opening circular slot on patch. In order to improve impedance matching further at high frequencies, two corners are tapered on the ground plane. Three antennas are produced to determine the repeatability of manufacturing and robustness of the design for manufacturing tolerances. All antennas have UWB

characteristics and 10dB bandwidth of 2.6 GHz-20 GHz is observed. The produced UWB ring monopole antenna has omnidirectional radiation pattern over the operating frequency band and cross-polarization is at low level from 3 to 11 GHz. Thus, the small size, simple geometry, and improved radiation characteristics make the proposed antenna a good candidate for UWB applications.

Second, the simple circular monopole antenna is modified by symmetrical open circuited stubs on ground plane. The aim is to distribute current in the symmetrical open circuited stubs, which can improve the radiation patterns of the antenna at high frequencies. The antenna is produced and tested. The fabricated antenna has the frequency band from 4.3 GHz to 11.2 GHz. However, it does not have good radiation pattern as UWB ring monopole antenna and cross polarization is high for frequencies greater than 8 GHz. The parallel strips on ground plane are close to patch antenna, which has interference with radiation pattern of monopole antenna. This may be the reason for poor radiation characteristics.

Finally, a microstrip line fed UWB monopole antenna with band notched characteristics is presented. U-shaped slot is etched on the feedline to obtain band notched characteristics at WLAN frequencies (5 GHz-6 GHz). The fabricated antenna has the frequency band from 2.5 GHz to 16.5 GHz with WLAN stopband frequency of 4.9-6.5 GHz.

It is seen that all of the presented antennas have almost omnidirectional patterns in UWB frequencies 3-11 GHz. There exist some differences between measured and simulated results due to fabrication errors, effect of SMA connectors and non-uniformity of dielectric constant.

Using substrate with small dielectric constant and loss tangent can increase the gain and efficiency of the antenna at high frequencies, which can be studied as a future work.

REFERENCES

[1] F. Mahmood, I. Mohsin, S. Ali, and A.Karim, "Design of an Ultra-Wideband Monopole Antenna for Handheld Devices," Asian Journal of Engineering, Sciences & Technology., vol. 1, no. 1, pp. 8-11,2011.

[2] O. Mrabet, "High Frequency Structure Simulator (HFSS) Tutorial", 2005

[3] X.Liang, "Ultra-Wideband Antenna and Design," Intech Open Access Publisher, 2012.

[4] S. Suh and S. Jazi, "A Comprehensive Investigation of New Planar Wideband Antennas," Virginia Polytechnic Institute and State University, 2002.

[5] N. Agrawall, G. Kumar and K. Ray, "Wide-Band Planar Monopole Antennas Narayan," IEEE Trans Antennas Propag., vol. 46, no. 2, pp. 294-295, 1998.

[6] S. Mishra, K. Gupta and J. Mukherjee1, "Parallel Metal-Plated Tuning Fork Shaped Omnidirectional Monopole Antenna for UWB Application," Microwave and Optical Technology Letters., vol. 53, no. 3, pp. 601-604, 2011.

[7] Y. Huang, K. Boyle, "Antennas from Theory to Practice", John Wiley & Sons Ltd., 2008.

[8] N. Sabbar, H. Asselman, S. Ahyoud, and A. Asselman, "Study of a Circular Monopole Antenna with T-shaped Slot in the Patch for Ultra-Wideband (UWB) Applications," International Journal of Innovation and Applied Studies., vol. 17, no. 1, pp. 169-175, 2016.

[9] J. Liang, C.C. Chiau, X. Chen and C.G. Parini, "Printed circular disc monopole antenna for ultra-wideband applications" Electronics Letters., vol. 40, no. 20, pp. 6-7, 2004.

[10] S. Rani, E. D. Singh and K. Sherdia, "UWB Circular Microstrip Patch Antenna Design Simulation & Its Analysis" International Journal of Advanced Research in Computer and Communication Engineering, vol. 3, no. 7, pp. 7519–7521, 2014.

[11] J. Liang, C. C. Chiau, X. Chen and C. G. Parini, "Study of a Printed Circular Disc Monopole Antenna for UWB Systems," IEEE Transactions on Antennas and Propagation, vol. 53, no. 11, pp. 3500–3504, 2005.

[12] P. Li, J. Liang and X. Chen, "Study of printed Elliptical/Circular Slot Antenna for Ultrawideband Applications," IEEE Transactions on Antennas and Propagation, vol. 54, no. 6, pp. 1670–1675, 2006.

[13] P.Trupti N.Pawase, R.P.Labade, "A Simple Compact UWB antenna with Band Notched Characteristics,"International Journal of Microwaves Applications, vol. 3, no.5, pp. 2772–2790, 2014.

[14] H.Liu, Z.Xu, B.Wu, J.Liao, "Compact UWB Antenna with dual-band notches for WLAN and WIMAX applications","Research Instutue of Electronic Science and Technology , vol. 1, no.5, pp. 1–6, 2013.

[15] Young Jun Cho, Ki Hak Kim, Dong Hyuk Choi, Seung Sik Lee, and Seong-Ook Park, "A Miniature UWB Planar Monopole Antenna With 5-GHz Band Rejection Filter and the Time-Domain Characteristics", IEEE Transactions On Antennas And Propagation, Vol. 54, No. 5, 1453-1460, 2006.

[16] R. P. Labade, N. Pishoroty, S.B.Deosarkar, A. R. Tambe, "A Very Compact Bandnotched UWB Monopole Antenna for Wireless Communication", 2015 IEEE Bombay Section Symposium (IBSS), Vol.1,No.4, 954-978, July, 2015.